Original Article

MOLECULAR METABOLISM

Raphe serotonin projections dynamically regulate feeding behavior through targeting inhibitory circuits from rostral zona incerta to paraventricular thalamus

Qiying Ye, Jeremiah Nunez, Xiaobing Zhang*

ABSTRACT

Objective: Rostral zona incerta (ZIR) evokes feeding by sending GABA transmission to paraventricular thalamus (PVT). Although central serotonin (5-HT) signaling is known to play critical roles in the regulation of food intake and eating disorders, it remains unknown whether raphe 5-HT neurons functionally innervate ZIR-PVT neural pathway for feeding control. Here, we sought to reveal how raphe 5-HT signaling regulates both ZIR and PVT for feeding control.

Methods: We used retrograde neural tracers to map 5-HT projections in Sert-Cre mice and slice electrophysiology to examine the mechanism by which 5-HT modulates ZIR GABA neurons. We also used optogenetics to test the effects of raphe-ZIR and raphe-PVT 5-HT projections on feeding motivation and food intake in mice regularly fed, 24 h fasted, and with intermittent high-fat high-sugar (HFHS) diet. In addition, we applied RNAscope in situ hybridization to identify 5-HT receptor subtype mRNA in ZIR.

Results: We show raphe 5-HT neurons sent projections to both ZIR and PVT with partial collateral axons. Photostimulation of 5-HT projections inhibited ZIR but excited PVT neurons to decrease motivated food consumption. However, both acute food deprivation and intermittent HFHS diet downregulated 5-HT inhibition on ZIR GABA neurons, abolishing the inhibitory regulation of raphe-ZIR 5-HT projections on feeding motivation and food intake. Furthermore, we found high-level 5-HT1a and 5-HT2c as well as low-level 5-HT7 mRNA expression in ZIR. Intermittent HFHS diet increased 5-HT7 but not 5-HT1a or 5-HT2c mRNA levels in the ZIR.

Conclusions: Our results reveal that raphe-ZIR 5-HT projections dynamically regulate ZIR GABA neurons for feeding control, supporting that a dynamic fluctuation of ZIR 5-HT inhibition authorizes daily food intake but a sustained change of ZIR 5-HT signaling leads to overeating induced by HFHS diet.

Keywords Zona incerta; Paraventricular thalamus; Raphe nuclei; Serotonin; Food intake

1. INTRODUCTION

Zona incerta (ZI) is a subthalamic brain area that has been recently found to participate in the regulation of feeding, sleep, anxiety, and curiosity [1–7]. To control eating behavior, inhibitory GABA neurons in the ZI send their projections to paraventricular thalamus (PVT) for initiating food intake and periaqueductal gray (PAG) for predatory hunting [3,4,8]. These latest evidences further explain why patients receiving deep brain stimulation of the subthalamus, including the ZI, for the treatment of movement disorders developed binge eating [9–11]. However, little is known how ZI neurons are regulated by neural signaling from other brain areas for the regulation of daily food intake as well as the involvement in the development of eating disorders.

Serotonin (5-HT) is a monoamine neurotransmitter that is produced by neurons located in both dorsal raphe (DR) and median raphe (MnR) nuclei of the brain stem [12]. Despite a restricted location only in raphe nuclei, 5-HT neurons send their projections widely to many brain areas for the regulation of emotion, reward, and motivated behaviors [13–18]. Especially, central 5-HT signaling plays an essential role in the regulation of feeding including both homeostatic and hedonic food intake [13]. Due to the diversity of 5-HT receptor subtypes expressed in neurons innervated by 5-HT neurons, 5-HT released by the synaptic terminals at different targets differentially regulate food intake. For example, stimulation of 5-HT projections inhibited homeostatic food intake by releasing 5-HT to activate both 5-HT2c and 5-HT1b receptors in the arcuate nucleus [13,19], while activation of 5-HT projections to

Department of Psychology, Florida State University, Tallahassee, FL 30304, USA

*Corresponding author. E-mail: xzhang@psy.fsu.edu (X. Zhang).

Abbreviations: DR, dorsal raphe; GAD67, glutamate decarboxylase 67; GABA, γ-Aminobutyric acid; HFHS, high-fat high-sugar; MnR, median raphe; PAG, periaqueductal gray; PBN, parabrachial nucleus; PR, progressive-ratio; PVT, paraventricular thalamus; 5-HT, serotonin; Sert, serotonin transporter; sEPSCs, spontaneous excitatory postsynaptic currents; vGAT, vesicular GABA transporter; VTA, ventral tegmental area; ZI, zona incerta; ZIR, rostral zona incerta

Received August 1, 2022 • Revision received November 2, 2022 • Accepted November 3, 2022 • Available online 10 November 2022

https://doi.org/10.1016/j.molmet.2022.101634

the ventral tegmental area (VTA) reduced hedonic eating through the action at 5-HT2c receptors [13,20]. However, activation of 5-HT2c in neurons of the paraventricular nucleus of the hypothalamus promoted feeding [21]. These findings suggest a complex role of central 5-HT system in the control of food intake due to brain-wide 5-HT projections. In addition, serotonergic neuroplasticity and changed 5-HT signaling have been reported for the development of brain dysfunctions such as alcohol addiction and eating disorders [22–26]. Both fasting and hyperphagia have also been found to alter the expression and the function of 5-HT1a, 5-HT1b, and 5-HT2c receptors in the brain [27–29]. For a better understanding about how central 5-HT signaling regulates eating behavior and the involvement in the development of eating disorders, it is critical to decipher specific 5-HT projections that target key brain areas for feeding control.

We recently reported that 5-HT activated PVT neurons through a direct depolarization via 5-HT7 receptors in these neurons and an indirect disinhibition mediated by an action on presynaptic 5-HT1a receptors in ZI-PVT inhibitory pathway [30]. Although we also found that PVT-projecting neurons were sensitive to the metabolic states revealed by retrograde neural tracing and food deprivation, direct evidence is required to confirm whether and how raphe-PVT 5-HT projections regulate food intake. In addition to PVT, ZI neurons were also reported to express 5-HT receptors such as 5-HT1a and 5-HT7 [31–33]. However, little is known whether raphe 5-HT neurons send projections to modulate rostral ZI (ZIR) GABA neurons for the regulation of feeding behavior. In the present study, we studied functional 5-HT neural circuits that connect to both ZIR and PVT for the regulation of feeding behavior in transgenic Sert-Cre mice using a combination of tools including neural circuit tracing, optogenetics, and electrophysiological recordings. We also revealed a pharmacological mechanism by which 5-HT receptor subtypes mediate a bidirectional modulation of 5-HT on ZIR neurons as well as a dynamic change of this modulation by acute metabolic signals and intermittent high-fat diet.

2. MATERIAL AND METHODS

2.1. Animals

C57BL/6 J (Strain #: 000664), Sert-Cre (Strain #:014554) [34], and vGAT-Cre (Strain #: 028862) [35] mice were purchased from the Jackson Laboratory and GAD-GFP mice were generously provided by Pradeep G Bhide lab at Florida State University [36]. All mice of both sexes were housed in a climate-controlled vivarium on a 12:12 h light/dark cycle and *ad libitum* access to food and water. All animals and experimental procedures in this study were approved by the Florida State University Institutional Animal Care and Use Committee. Ketamine (100 mg/kg) plus xylazine (10 mg/kg) were used for anesthesia and meloxicam (5 mg/kg) was used for reducing pain or discomfort at the time of survival surgery and at least 2–3 days following the surgery. For brain slice preparation, mice were sacrificed with an overdose of ketamine (300 mg/kg) and xylazine (30 mg/kg).

2.2. Drugs

AS19 (#1968), SB242084 (2901/10), SB269970 (#1612/10), SB258585 (#1961/10), WAY100635 (#4380), 8-OH-DPAT (#0529/10), WAY629 (#2173), 5-Carboxamidotryptamine meleate (5-CT, #0458), D-2-amino-5-phosphonovalerate (AP5, #0106), bicuculline methiodide (Bic, #2503), and 6-Cyano-7-nitroquinoxaline-2,3-dione (CNQX, #0190) were purchased from Tocris Bioscience. Serotonin hydrochloride (5-HT, #H9523) was obtained from Sigma–Aldrich. All drugs were dissolved in water or DMSO and aliquoted as stock solutions that were stored at −80 °C. On the day of recording, the stock solutions were diluted to final concentrations in ACSF (at least 1:1000 dilution) for the experimental test. For experiments when DMSO was used for preparing stock solutions of some drugs (AS19, SB242084, and CNQX), we also added 0.1% of DMSO in ACSF of control condition. During the recording, drugs were delivered locally via a multi-channel drug application system (Warner Instruments, CT, USA) with a flow pipette of 250-μM diameter so that the drug solutions were quickly washed out after the drug channel was switched to normal ACSF.

2.3. Stereotactic injection of viral vectors and CTB-555

Naïve male and female mice of 8–10 weeks old were anesthetized with intraperitoneal injections of ketamine (100 mg/kg) and xylazine (10 mg/kg) and placed on a stereotaxic apparatus (David Kopf Instruments, CA, USA). Meloxicam (5 mg/kg) was also given for reducing pain or discomfort before the surgery and the following 2–3 days. After exposing the skull via a small incision and drilling a hole in the skull, a pulled-glass pipette with beveled tip of 20–40 μm diameter was inserted into the brain to target DR (coordinates relative to bregma, AP: −4.36 mm, DV: −3.00 mm, ML: ±0.05 mm) and MnR (AP: −4.36 mm, DV: −4.25 mm, ML: ±0.05 mm) for injection of AAV1-EF1a-DIO-ChR2(H134R)-EYFP-WPRE-HGHpA (500 nl, from Addgene, Cat#: 20298-AAV1), AAV-pCAG-FLEX-EGFP-WPRE (500 nl, from Addgene, Cat#: 51505-AAV1) or AAV1-EF1a-DIO-EYFP (500 nl, from Addgene, Cat#: 27056-AAV1) with a speed of 100 nl per min using a pressure pump. The pipette was slowly withdrawn 10 min after injection. Mice were returned to their home cages for recovery. At least 3 weeks after surgery to allow Cre-dependent protein expression, mice received a second surgery to implant fiber optics that target PVT (AP: −1.50 mm, DV: −2.80 mm, ML: ±0.05 mm) or ZIR (AP: −1.30 mm, DV: −4.20 mm, ML: ±0.70 mm). Two weeks after implantation of fiber optics, mice will be ready for behavioral experiments.

For retrograde labeling of PVT-projecting ZIR neurons for electrophysiological recording, cholera toxin subunit B conjugated with Alexa Fuor 555 (CTB-555, 200 nl, obtained from ThermoFisher Scientific, Cat#: C34776) was injected into PVT (coordinates relative to bregma, AP: −1.40 mm, DV: −3.00 mm, ML: ±0.05 mm) of GAD-GFP mice. 3–5 days after injection, mice were ready for patch-clamp recording and anatomical identification.

For retrograde tracing of 5-HT neurons that project to ZIR and PVT, AAVrg-CAG-FLEX-EGFP-WPRE (250 nl, from Addgene, #: 51502-AAVrg) was injected into the ZIR (AP: AP: −1.00 mm, DV: −4.50 mm, ML: ±0.70 mm) and AAVrg-CAG-FLEX-tdTomato-WPRE (250 nl, from Addgene, #: 28306-AAVrg) was injected into the PVT (AP: AP: −1.40 mm, DV: −3.00 mm, ML: ±0.05 mm) of the same Sert-Cre mice. 4 weeks after injections, mice were perfused for anatomical imaging.

2.4. Immunocytochemistry

Mice were anesthetized with ketamine (300 mg/kg, IP) and xylazine (30 mg/kg, IP), and then perfused transcardially with saline followed by 4% paraformaldehyde (PFA) in PBS solution. Brains were postfixed overnight in 4% PFA and then in 30% sucrose for 2 days. The 30-μM-thick coronal sections were cut using a cryostat and collected in PBS. Free-floating slices were washed three times for 10 min in PBS and incubated in a goat anti-serotonin antibody (1:2000, cat. #: 20079, ImmunoStar, Hudson, WI, USA) or rabbit anti-GABA antibody (1:1000, cat. #: PA5-32241, Invitrogen, Waltham, MA, USA) in PBS with 2% normal donkey serum at 4 °C overnight. After being washed three times for 10 min in PBS, sections were incubated in donkey anti-goat Cy3 (1:500, cat. #: 705165147, Jackson ImmunoResearch Laboratories, West Grove, PA, USA) or donkey anti-rabbit Cy3 (1:500, cat. #:

711165152, Jackson ImmunoResearch Laboratories, West Grove, PA, USA) for 4 h at room temperature. Sections were then washed in PBS for 3 times (10 min each time) and mounted on glass slides for imaging under microscope.

2.5. Slice preparation and patch-clamp recording

Coronal brain slices (300 μm thick) containing the ZI and PVT were prepared for patch-clamp recordings. After recovery of over 1 h from slicing, brain sections were transferred to a recording chamber mounted on a Zeiss upright microscope (Zeiss, Berlin, Germany) and perfused with a continuous flow of gassed artificial cerebrospinal fluid (ACSF) solution containing (in mM) 124 NaCl, 3 KCl, 2 $MgCl_2$, 2 $CaCl_2$, 1.23 NaH_2PO_4, 26 $NaHCO_3$, and 10 glucose (gassed with 95% O_2/5% CO_2; 300–305 mOsm). Pipettes used for whole-cell recording had resistances ranging from 4 to 7 MΩ when filled with K-gluconate pipette solution containing (in mM) 145 potassium gluconate, 1 $MgCl_2$, 10 HEPES, 1.1 EGTA, 2 Mg-ATP, 0.5 Na_2-GTP, and 5 disodium phosphocreatine (pH 7.3 with KOH; 290–295 mOsm). The recording was performed at 33 ± 1 °C using a dual-channel heat controller (Warner Instruments, Holliston, MA, USA). EPC-10 patch-clamp amplifier (HEKA Instruments, NY, USA) and PatchMaster 2 × 90.5 software (HEKA Elektronik, Lambrecht/Pfalz, Germany) were used to acquire and analyze the data. For voltage-clamp recording, the membrane potentials were held at −70 mV for recording membrane currents. Traces were processed using Igor Pro 6.37 (Wavemetrics, OR, USA). The postsynaptic currents were analyzed with MiniAnalysis 6.03 (Synaptosoft Inc., GA, USA).

2.6. Optogenetic stimulation

To photostimulate ChR2-positive axons, blue light (470 nm) was delivered to target ZIR or PVT through an optical fiber from a laser for both slice recordings and behavioral tests. The regular laser pulses (10 ms) of 20 Hz were controlled with an optogenetics TTL pulse generator (Doric lenses, Canada) to generate photostimulation-evoked currents.

2.7. Progressive-ratio (PR) schedule of reinforcement

Before operant conditioning training in mouse operant chambers (Med Associates, VT, USA), all mice were food-restricted (70% of their daily food intake) to facilitate the acquisition of lever-press responding until they learned to press the lever to obtain the food pellet in 3–5 days. Mice were provided with their daily quota of food in the home cage after termination of the training session. During the training, mice were initially trained under fixed-ratio 1 (FR1) sessions for 45 min daily during light cycles. Animals had a choice between two levers: an active lever press associated with a 3 s light cue with concomitant delivery of high-fat high-sugar (HFHS) pellets (Cat #S07687: 20 mg each pellet, 4.97 kcal/g, 48.9% kcal as fat and 34.6% as sucrose, Bio Serv, NJ, USA), and an inactive lever press that remained inoperative and served as a control for general activity. Each active lever press triggered the delivery of one pellet during FR1 sessions. The active lever had a 5 s refractory period after each food delivery so that mice could retrieve the single pellet but not drive supplementary food delivery. After a training period of about 7–10 days when three successive sessions of obtaining equal to or more than 20 pellets during the FR1 session of 45 min, mice were then engaged in consecutive 45-min PR sessions during light cycles (11:00 am–5:00 pm). For the PR session, the number of lever presses required for one food pellet delivery followed the order (calculated by formula $[5e^{(R*0.2)}]-5$ where R is equal to the number of food rewards already earned plus 1): 1, 2, 4, 6, 9, 12, 15, 20, and so on [37]. The maximal number of active lever presses performed to reach the final ratio was defined as the breakpoint, a value reflecting animals' motivation to obtain the food reward. When a relatively stable breakpoint was reached, mice were ready for PR tasks with or without photostimulation.

2.8. Intermittent HFHS diet manipulation

To target ZIR GABA neurons, we injected AAV1-EF1a-DIO-EYFP into ZIR of vGAT-Cre mice to selectively label ZIR GABA neurons for slice recordings. One month after virus injection, mice were assigned to two groups for diet manipulation. Mice in control group were regularly fed with normal diet (Cat #: 5001, 3.36 kcal/g, 13.50% kcal as fat and 5.80% as sucrose, LabDiet). However, mice in intermittent HFHS diet group maintained with normal diet for most of time but were treated with HFHS diet (Cat #: D12492, 5.21 kcal/g containing 60.0% kcal as fat and 20.0% kcal as sucrose, Research Diets Inc.) 2 h daily for 2–3 weeks before slice recordings and behavioral PR tests. For slice recordings, mice were sacrificed immediately before the scheduled HFHS food access of the day. For PR experiments, mice were put into operant chambers for the tests right before HFHS diet treatment each day.

2.9. HFHS food intake

HFHS food intake was measured over 30 min when mice were tethered to a laser for photostimulation. After mice were habituated to patch cord tethering for 3–5 days, they were ready for the food intake tests with or without photostimulation (20 Hz) delivered by a laser via an optogenetics TTL pulse generator (Doric lenses, Canada).

2.10. RNAscope in situ hybridization for identification of 5-HT receptor subtypes

We followed a RNAscope protocol validated by previous studies [38]. Briefly, free-floating brain sections (30 μm) containing the ZI were rinsed for 1 h in several changes in PB, treated with H_2O_2 (RNAscope reagent 322355, Advanced Cell Diagnostics) for 30 min at room temperature (RT) with light shaking, then rinsed for 30 min in changes of PB at RT. Sections were then mounted onto Globe Scientific Diamond White slides (cat. #: 89500-496, VWR) in 0.01 M Tris buffer solution, pH 7.3, air dried for 1 h, dipped into 100% ethanol (10 s), and air dried for 30 min. A hydrophobic barrier was created around sections and air dried overnight. Sections were treated with Protease IV (RNAscope reagent 322336, Advanced Cell Diagnostics) for 30 min at RT followed by 3 × 3 min rinses in distilled water. Sections were immediately processed using Advanced Cell Diagnostics probes for 5-HT1a (Mm-Htr1a; cat. #: 312301), 5-HT2c (Htr2c-C2; cat. #: 401001-C2), or 5-HT7 (Mm-Htr7-C3; cat. #: 401321-C3) as described below. Single labeling of 5-HT1a, 5-HT2c, or 5-HT7 receptor mRNA was detected using RNAscope Multiplex Fluorescent Reagent Kit v2 (cat. #: 323100, Advanced Cell Diagnostics) according to manufacturer instructions and using kit components. Sections were incubated with the corresponding probe for 2 h at 40 °C in a HybEZ II oven, followed by amplification steps 1–3, HRP incubation, and final labeling using Opal 570 (cat. #: FP1488001KT; Akoya Biosciences) and DAPI (cat. #: 323108, Advanced Cell Diagnostics) before coverslipping. Sections were washed 3 × 3 min in wash buffer (cat. #: 310091) at RT between each step. After the labeling reaction, sections were air dried and coverslipped using ProLong Gold Antifade (cat. #: P36930; Invitrogen). Images were acquired using Olympus BX53 LED fluorescent microscope at 10× and 20× magnification with the same criteria including exposure time and gain value for all samples. The ZIR areas were defined for qualitative imaging analysis based on the Allen Mouse Brain Atlas and our previous experience in studying this area for feeding

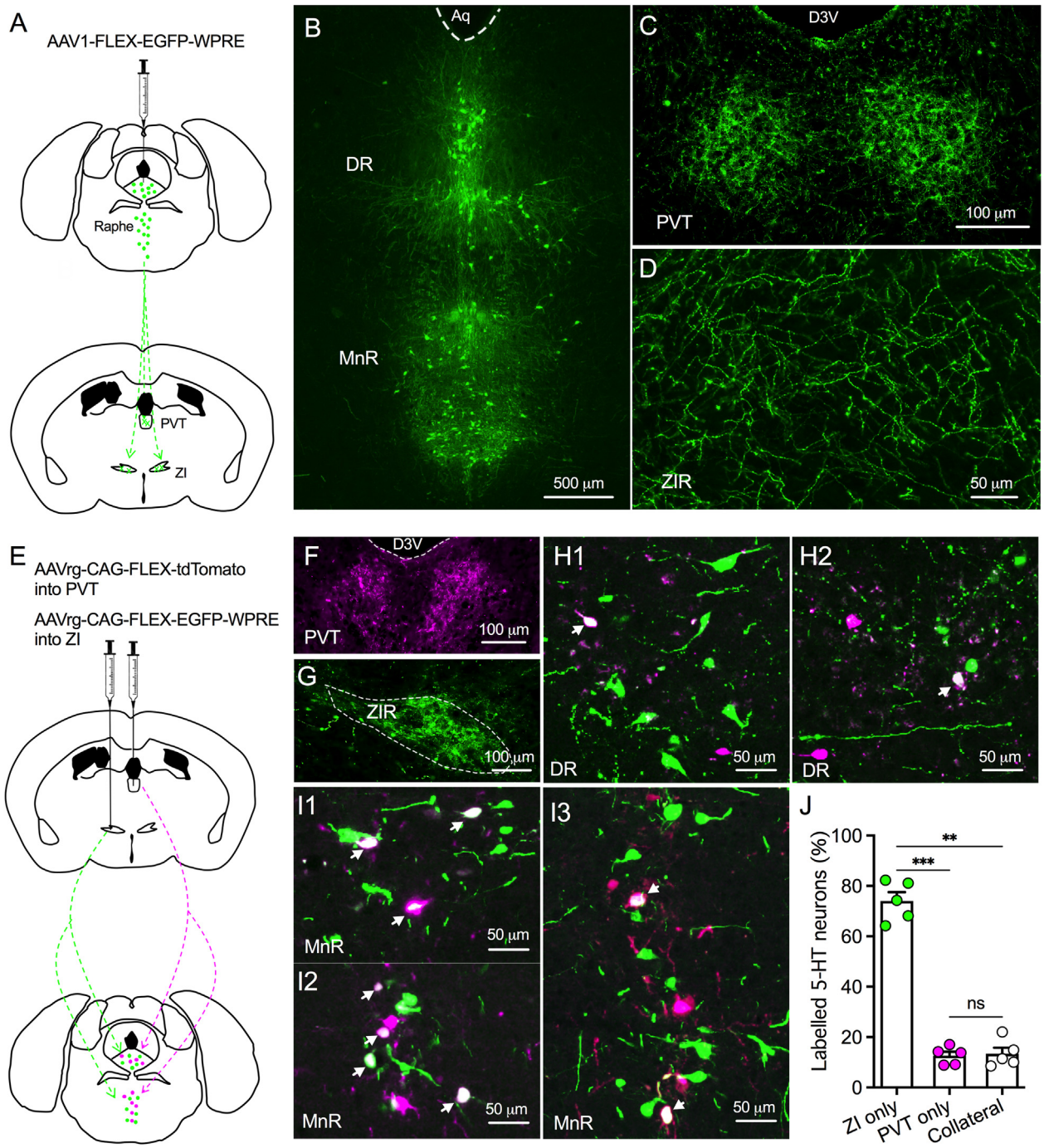

Figure 1: 5-HT neurons project to ZIR and PVT with collateral axons. A, A diagram shows AAV1-FLEX-EGFP-WPRE was injected into both DR and MnR of Sert-Cre mice for tracing 5-HT projections. B, A representative image showing EGFP-positive neurons in both DR and MnR. C, Dense EGFP-positive axons were detected in PVT. D, A representative image showing EGFP-positive axons in ZIR. E, A diagram shows that AAVrg-CAG-FLEX-tdTomato was injected into PVT and AAVrg-CAG-FLEX-EGFP-WPRE was injected into ZIR of Sert-Cre mice for retrogradely mapping raphe 5-HT neurons that project to both PVT and ZI. F, A representative image showing tdTomato-positive terminals in PVT. G, A representative image showing GFP-positive terminals in ZIR. H1—H2, Representative images showing both GFP- and tdTomato-positive neurons in DR. I1—I3, Representative images showing both GFP- and tdTomato-positive neurons in MnR. J, A bar graph showing ZI-projecting only, PVT-projecting only, and collateral-projecting 5-HT neurons in raphe nuclei from 5 mice. $F_{(1.155,4.621)} = 119.4$, $p = 0.0002$; ns, no significance, $^{***}p < 0.001$, One-way ANOVA followed by Bonferroni's comparisons test.

regulation [3]. To determine the density of the image signals and the average intensity of all signal dots, we used Fiji [39], an open-sourced program developed by the NIH, for quantitative analysis with a threshold value set to select real signals from background noise followed the guideline from Advanced Cell Diagnostics. The threshold setting stayed unchanged across all images for the measurement and analysis. mRNA signal density was calculated as the signal area divided by the area of interest (ZIR in this study) [40].

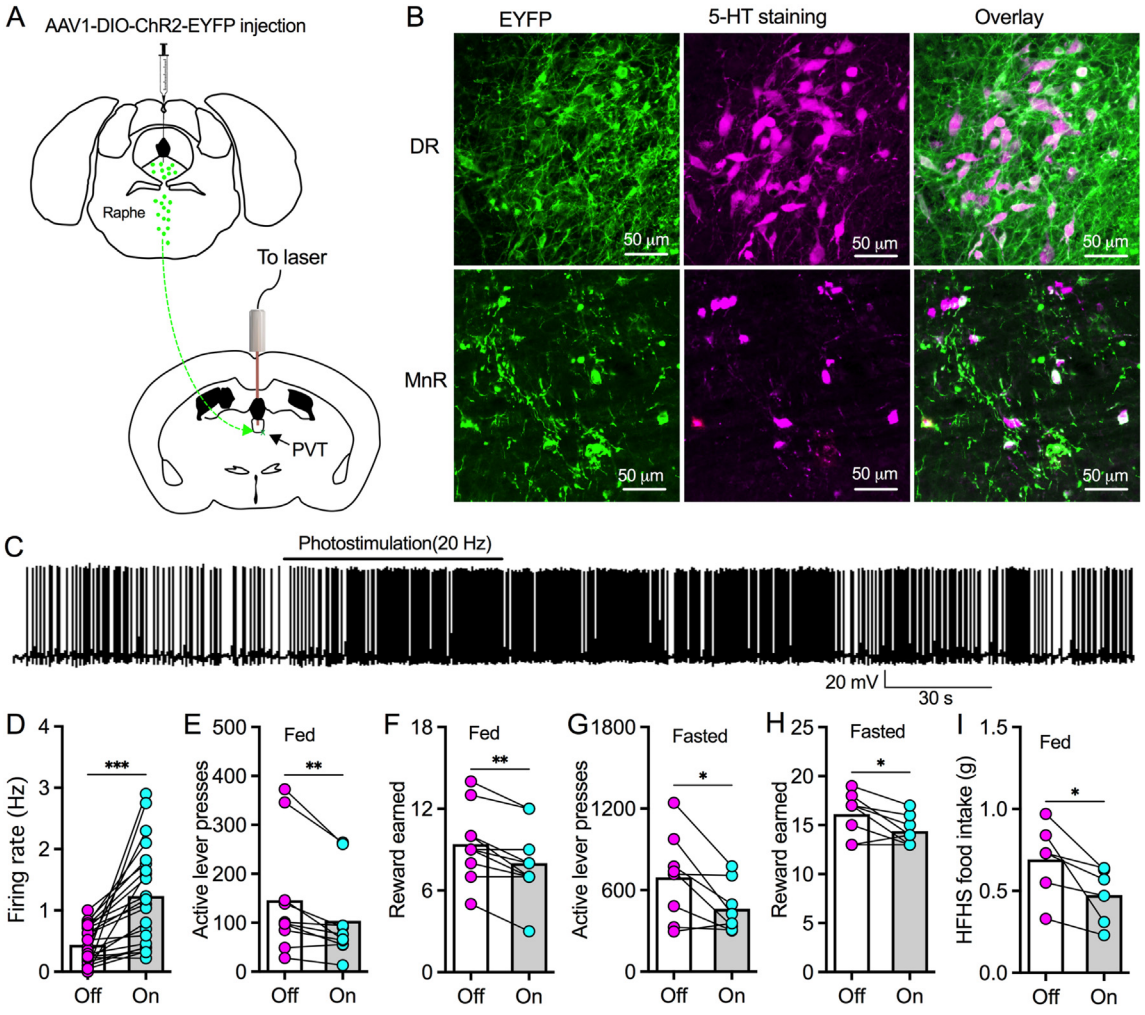

Figure 2: Photostimulation of raphe-PVT 5-HT projections excites PVT neurons and reduces food motivation. A, A diagram showing AAV1-DIO-ChR2-EYFP was injected into both DR and MnR of Sert-Cre mice. Fiber optics were implanted to target PVT for photostimulation. B, ChR2-EYFP-positive (left) and 5-HT immunoreactive (middle) neurons were found to be colocalized (right) in both DR (above) and MnR (bottom). C, A representative trace showing photostimulation (20 Hz) of raphe-PVT 5-HT axonal terminals excited a PVT neuron from a Sert-Cre mouse with AAV1-DIO-ChR2-EYFP injection into raphe nuclei. D, Bar graph with data plots showing photostimulation (20 Hz) of raphe-PVT 5-HT projections increased firing rate of PVT neurons. $^{***}p < 0.001$, n = 22 neurons, paired *t* test. E, Photostimulation of raphe-PVT 5-HT projections reduced active lever presses for HFHS pellets of regularly fed mice during a 45-min PR session. $^{**}p < 0.01$, n = 10 mice, paired *t* test. F, Photostimulation of raphe-PVT 5-HT projections decreased HFHS reward retrieval in regular fed mice during a 45-min PR session. $^{**}p < 0.01$, n = 10 mice, paired *t* test. G, Photostimulation of raphe-PVT 5-HT projections reduced active lever presses for HFHS pellets of 24-h fasting mice during a 45-min PR session. $^{*}p < 0.05$, n = 8 mice, paired *t* test. H, Photostimulation of raphe-PVT 5-HT projections decreased HFHS reward retrieval in 24-h fasting mice earned during a 45-min PR session. $^{*}p < 0.05$, n = 8 mice, paired *t* test. I, Photostimulation (20 Hz) of raphe-PVT 5-HT projections decreased HFHS food consumption over 30 min $^{*}p < 0.05$, n = 6 mice, paired *t* test.

2.11. Statistical analysis

Data are expressed as mean ± SEM. Statistical significance was assessed using a two-sided Student's *t*-test and Chi-squared test for comparison of two groups, and one-way, or two-way ANOVA followed by a Bonferroni *post hoc* test for three or more groups. Prism 9 (GraphPad, CA, USA) was used for statistical analysis and figure making.

3. RESULTS

3.1. 5-HT neurons send projections to both ZIR and PVT with collateral axons

To examine whether raphe 5-HT neurons project to both ZIR and PVT, we first injected AAV1-FLEX-EGFP-WPRE into both DR and MnR of Sert-Cre mice for labelling raphe 5-HT neurons and their axonal terminals with EGFP expression (Figure 1A). We found EGFP was only expressed in raphe 5-HT neurons (Figure 1B) and dense EGFP-positive terminals were detected in both PVT and ZIR (Figure 1C,D). These data thus show raphe 5-HT neurons send their projections to innervate both ZIR and PVT neurons. To reveal the exact location of 5-HT neurons that project to both ZIR and PVT, we injected AAVrg-CAG-FLEX-tdTomato into PVT and AAVrg-CAG-FLEX-EGFP-WPRE into ZIR of Sert-Cre mice for retrograde tracing of raphe 5-HT neurons (Figure 1E). Dense tdTomato-positive axons were found in PVT and GFP-positive axons were detected in ZIR from presynaptic raphe 5-HT neurons (Figure 1F,G). Furthermore, we found both tdTomato-positive and EGFP-positive neurons in raphe nuclei including DR (Figure 1H1—H2) and MnR (Figure 1I1-I3). Interestingly, 5-HT neurons with tdTomato and EGFP colocalization were detected in both DR and MnR (Figure 1H1-I3). In all retrogradely labelled neurons in both DR and

MnR, we found 74.0 ± 3.5% of neurons expressed GFP only, 12.6 ± 1.6% of neurons expressed tdTomato only, and 13.4 ± 2.4% neurons were co-expressed with both tdTomato and EGFP from 5 mice (Figure 1J). Together, these data suggest that a small population of ZIR-projecting raphe 5-HT neurons collaterally innervate PVT. However, a half of PVT-projecting raphe 5-HT neurons send collateral axons to ZIR.

3.2. Optogenetic activation of raphe-PVT 5-HT pathway excites PVT neurons to depress food motivation and consumption

In a latest study of ours, we reported that 5-HT directly depolarizes PVT neurons through activating 5-HT7 receptors and decreased GABA transmissions from ZI to PVT by binding to 5-HT1a receptors in GABAergic synaptic terminals [30]. Based on our findings about the pharmacological modulation of 5-HT and 5-HT projections to PVT, we asked whether raphe 5-HT projections functionally regulate PVT neurons. To answer this question, we injected AAV1-DIO-ChR2-EYFP into raphe nuclei of Sert-Cre mice to induce ChR2 expression selectively in raphe 5-HT neurons for photostimulation of 5-HT terminals in PVT (Figure 2A). Neurons in DR and MnR with virus-induced ChR2-EYFP expression were stained with 5-HT immunoreactivity (Figure 2B), confirming that ChR2 was only expressed in raphe 5-HT neurons. We then recorded the activity of PVT neurons innervated by ChR2-positive terminals in PVT of slices and found photostimulation (20 Hz) increased firing rates to excite PVT neurons (Figure 2C,D). We also found that photostimulation of ChR2-positive 5-HT axons depressed the frequency of GABAergic inhibitory postsynaptic currents (IPSCs) on PVT neurons (Supplementary Figure 1), further corroborating that PVT 5-HT signaling also disinhibits PVT neurons by targeting inhibitory synaptic transmissions possibly from ZIR GABA neurons [30]. Our last studies reported that PVT-projecting DR neurons were inhibited by overnight fasting [30], suggesting raphe-PVT 5-HT projections are involved in the control of food intake. To examine whether raphe-PVT 5-HT projections regulate motivation for food, we tested the effect of photostimulation of PVT 5-HT terminals on operant behaviors for food reward using a progressive-ratio (PR) schedule of reinforcement. We found photostimulation of raphe-PVT 5-HT projections decreased active lever presses to obtain high-fat high-sugar (HFHS) food reward in both regularly fed (Figure 2E,F) and 24-h fasted mice (Figure 2G,H). Furthermore, we found photostimulation of raphe-PVT 5-HT projections decreased HFHS food intake over 30 min in home cages (Figure 2I). Together, these data indicate that activation of raphe-PVT 5-HT pathway inhibits food motivation to decrease palatable food consumption.

3.3. Optogenetic activation of raphe-ZIR 5-HT projections inhibits ZIR neurons to decrease food motivation and consumption

To examine whether and how raphe 5-HT projections regulate ZIR neurons and feeding behavior, we similarly injected AAV1-DIO-ChR2-EYFP or AAV1-DIO-EYFP into raphe nuclei of Sert-Cre mice to induce ChR2-EYFP or EYFP expression selectively in raphe 5-HT neurons for recording of ZIR neurons innervated by ChR2-positive 5-HT terminals (Figure 3A). In freshly prepared slices, we recorded the activity of ZIR neurons innervated by ChR2-positive 5-HT terminals. In control mice with EYFP expression in 5-HT neurons, photostimulation (20 Hz) produced little effect on firing rates and membrane potentials of ZIR neurons (Figure 3B—D). However, photostimulation decreased firing rates and hyperpolarized membrane potentials of ZIR neurons from mice with ChR2-EYFP expression in 5-HT neurons (Figure 3B—D). Thus, these data indicate that optogenetic activation of raphe-ZIR 5-HT projections inhibits a majority of ZIR neurons.

To further test the effect of raphe-ZIR photostimulation on motivation for HFHS food, we injected AAV1-DIO-ChR2-EYFP or AAV1-DIO-EYFP into raphe nuclei to induce ChR2-EYFP or EYFP expression in 5-HT neurons (Figure 3E) and implanted fiber optics to target ZIR for photostimulation in Sert-Cre mice (Figure 3E,F). Photostimulation (20 Hz) of raphe-ZIR 5-HT terminals decreased active lever presses to reduce breakpoints for HFHS food reward without an effect on inactive lever presses in mice with ChR2-EYFP in raphe 5-HT neurons during PR trials (Figure 3G—J). Photostimulation of raphe-ZIR 5-HT terminals in mice with ChR2-EYFP expression in 5-HT neurons also decreased home-cage HFHS food consumption over 30 min (Figure 3K). However, we did not observe an obvious effect of photostimulation on food reward earned during PR trials in control mice with EYFP expression in raphe 5-HT neurons (Figure 3L). Together, these data suggest that optogenetic activation of raphe-ZIR 5-HT projections inhibits motivation for food consumption.

3.4. 5-HT exerts bidirectional modulation on ZIR neurons but predominantly inhibits PVT-projecting GABA neurons

Our latest findings indicated that 5-HT decreases GABA release from ZI GABAergic terminals in PVT. To examine whether 5-HT also modulates the activity of ZI GABA neurons that project to PVT, we first tested the effect of 5-HT on ZIR neurons in C57BL/6 J mice (Supplementary Figure 2). We found 5-HT (50 μM) treatment for 1 min produced multiple effects on ZIR neurons in the absence of synaptic blockers: inhibitory only (48.6% of recorded neurons), inhibitory followed by excitatory during washout (17.1% of 35 recorded neurons), excitatory only (34.3% of recorded neurons) (Figure 4A—C). The inhibitory effects of 5-HT normally lasted for 1—2 min after washout (Figure 4A). However, the excitatory effects were normally delayed and could last more than 5 min after washout (Figure 4A). These data suggest that the complex effect of 5-HT is mediated by differential combinations of 5-HT receptor subtypes in ZIR neurons. We then tested 5-HT effect in the presence of synaptic blockers (AP5: 50 μM; CNQX: 10 μM; and Bic: 30 μM). Similarly, we found 5-HT (50 μM) inhibited 55.5%, inhibited followed by excited 16.7%, and excited 27.8% of 18 recorded neurons (Figure 4D,E). Pooling all data together, we found 5-HT (50 μM) inhibited 50.9%, inhibited followed by excited 17.0%, and excited 32.1% of 53 recorded neurons (Figure 4F).

Next, we tested whether 5-HT modulates the activity of PVT-projecting ZIR GABA neurons. CTB-555 was injected into PVT of GAD-GFP mice to label presynaptic neurons in ZIR (Figure 4G—I). As we reported previously, we found high-density of CTB-positive GAD-GFP neurons in ZIR (Figure 4I1—I3). Furthermore, we recorded the activity of ZIR CTB-positive GAD-GFP neurons in slices (Figure 4J). 5-HT (50 μM) treatment for 1 min significantly hyperpolarized 14 neurons recorded (Figure 4K). However, we also observed 2 of 14 neurons had increased firing rate during treatment and 3 of 14 neurons were initially inhibited by 5-HT during treatment but then excited during washout (Figure 4L). Although these data showed a bidirectional modulation, 5-HT predominantly produced an inhibitory effect on PVT-projecting ZIR GABA neurons.

3.5. Multiple 5-HT receptor subtypes competitively mediate a bidirectional 5-HT modulation on ZIR neurons

To determine what 5-HT receptor subtypes contribute to bidirectional 5-HT modulation, we pharmacologically tested the effects of various 5-HT subtype agonists on ZIR neurons of slices. 5-CT was used as a selective agonist for 5-HT1a receptor though it was found to activate other 5-HT receptor subtypes such as 5-HT2c and 5-HT7. Here, we first tested the effect of 5-CT on the activity of ZIR neurons. Unlike 5-

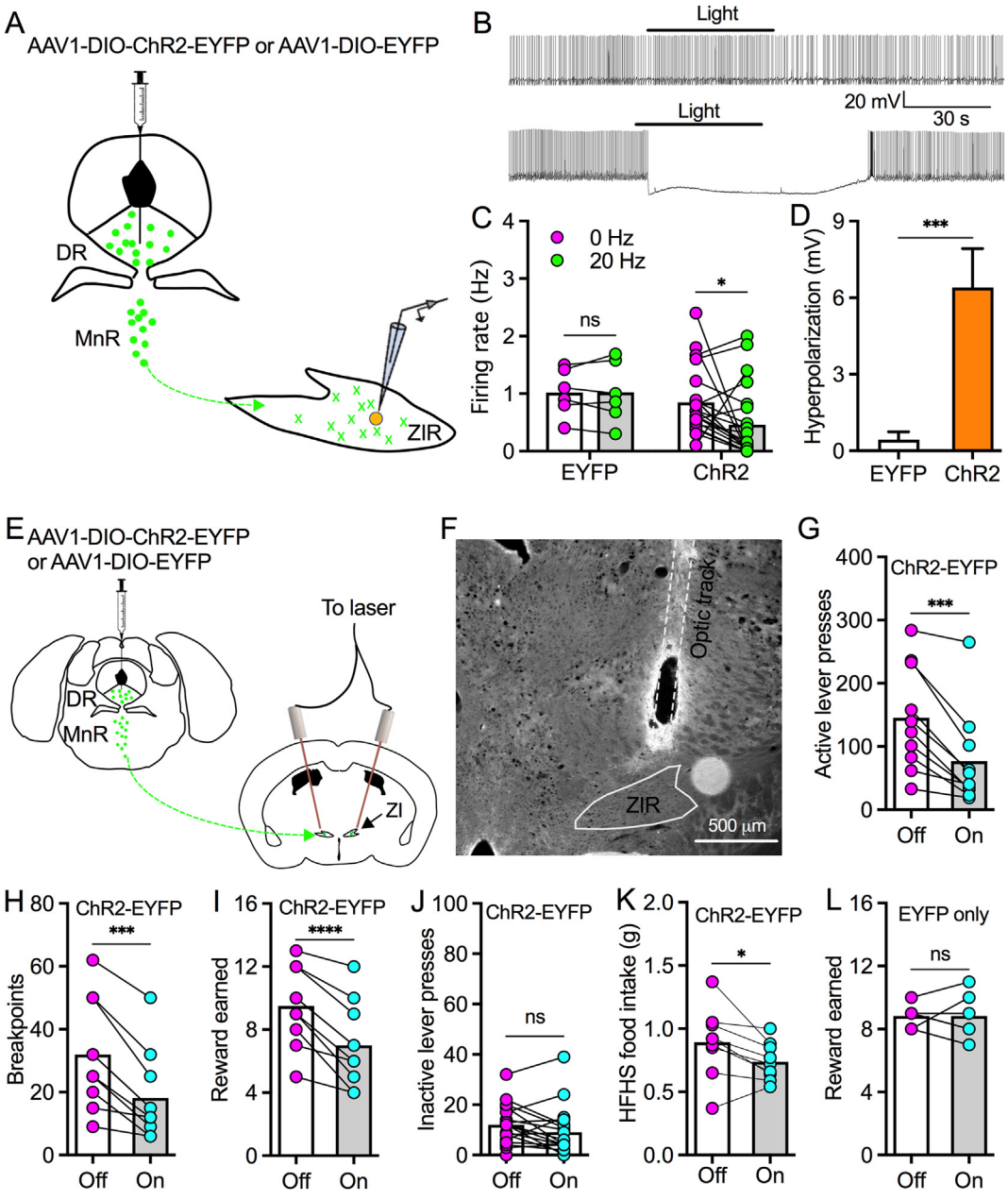

Figure 3: Photostimulation of raphe-ZIR 5-HT projections inhibits ZIR neurons and food motivation. A, A diagram showing AAV1-DIO-ChR2-EYFP or AAV1-DIO-EYFP was injected into both DR and MnR of Sert-Cre mice. Patch-clamp recordings were performed on ZIR neurons innervated by ChR2-positive axonal terminals. B, Representative traces showing photostimulation (20 Hz) had no effect on the activity of a ZIR neuron (top) in a control mouse with EYFP expression in raphe 5-HT neurons, but inhibited a ZIR neuron (bottom) in a mouse with ChR2-EYFP expression in raphe 5-HT neurons. C, Bar graph with data plots indicates that photostimulation decreased the firing rate of ZIR neurons innervated by ChR2-positive 5-HT terminals but not by EYFP-positive terminals. ns, no significance, $^{*}p < 0.05$, n = 6 neurons from control mice with EYFP expression in raphe 5-HT neurons, 21 neurons from mice with ChR2-EYFP expression in raphe 5-HT neurons, two-way ANOVA followed by Bonferroni's comparisons test. D, Bar graph shows that photostimulation induced hyperpolarization in ZIR neurons. $^{***}p < 0.001$, n = 6 neurons from control mice with EYFP expression in raphe 5-HT neurons and 21 neurons from mice with ChR2-EYFP expression in raphe 5-HT neurons, Unpaired t test. E, A diagram showing the strategy for AAV1-DIO-ChR2-EYFP or AAV1-DIO-EYFP injection into raphe nuclei and implantation of fiber optics to target ZIR of Sert-Cre mice. F, A representative image shows the fiber optic track that targets ZIR for photostimulation. G, Photostimulation of raphe-ZIR 5-HT projections decreased active lever presses for HFHS pellets during a 45-min PR session in mice with ChR2-EYFP expression in raphe 5-HT neurons. $^{***}p < 0.001$, n = 10 mice, paired *t* test. H, Photostimulation of raphe-ZIR 5-HT projections decreased breakpoints for HFHS pellets during a 45-min PR session in mice with ChR2-EYFP expression in raphe 5-HT neurons. $^{***}p < 0.001$, n = 10 mice, paired *t* test. I, Photostimulation of raphe-ZIR 5-HT projections reduced HFHS pellet retrieval during a 45-min PR session in mice with ChR2-EYFP expression in raphe 5-HT neurons. $^{****}p < 0.0001$, n = 10 mice, paired *t* test. J, Photostimulation of raphe-ZIR 5-HT projections produced no effect on inactive lever presses during a 45-min PR session in mice with ChR2-EYFP expression in raphe 5-HT neurons. ns, no significance, paired *t* test. K, Photostimulation (20 Hz) of raphe-ZIR 5-HT projections decreased HFHS food consumption over 30 min in mice with ChR2-EYFP expression in raphe 5-HT neurons. $^{*}p < 0.05$, n = 9 mice, paired *t* test. L, Photostimulation of raphe-ZI 5-HT projections produced no effect on HFHS pellet retrieval during a 45-min PR session in control mice with EYFP expression in raphe 5-HT neurons. ns, no significance, n = 6 mice, paired *t* test.

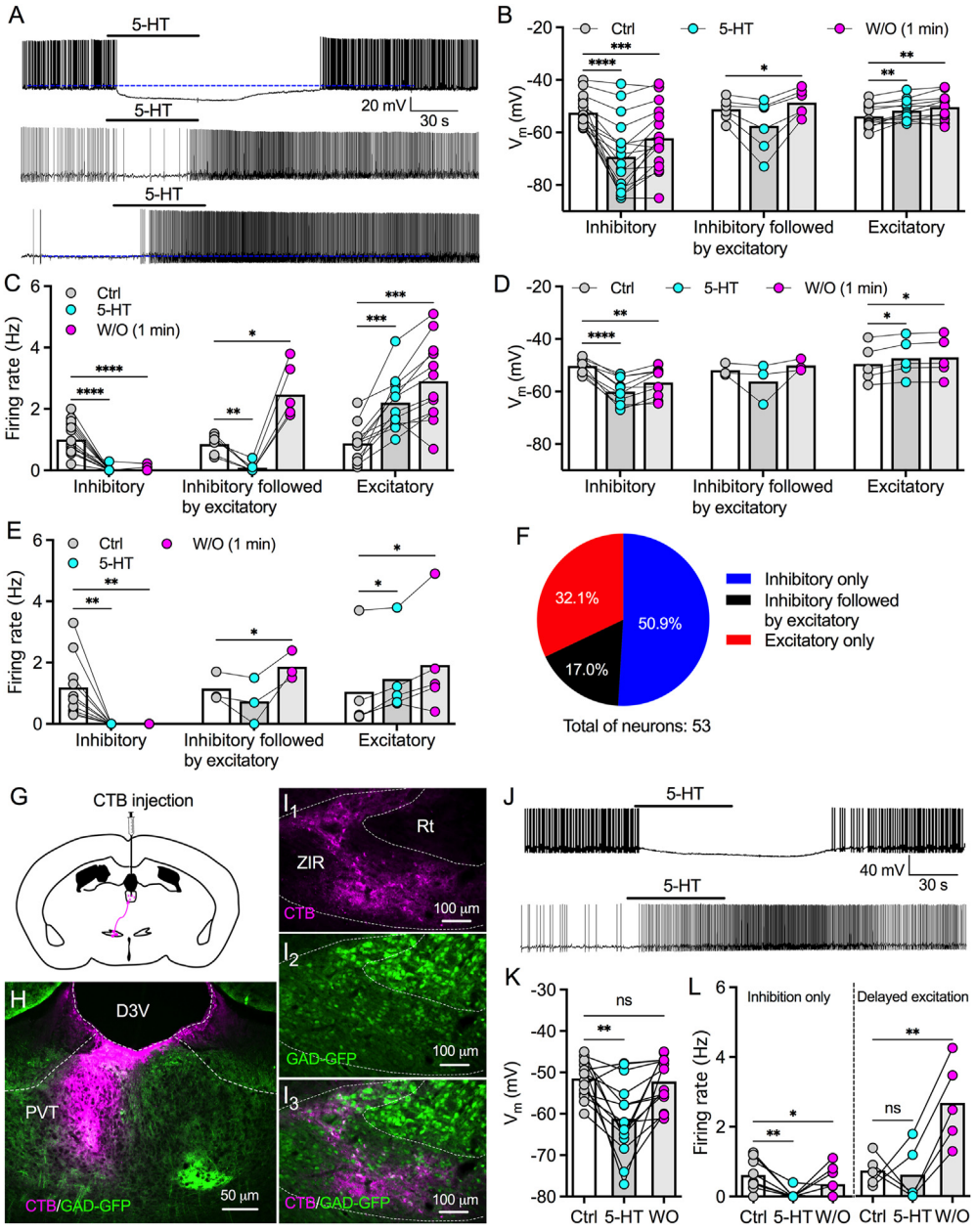

Figure 4: 5-HT predominantly decreases the activity of PVT-projecting GABA neurons. A, Representative traces shows inhibitory, inhibitory followed by excitatory, or excitatory effect of 5-HT on the activity of three different ZIR neurons in the absence of synaptic blockers. B, 5-HT induced membrane potential changes during 5-HT treatment and washout of 1 min in three different types of ZIR neurons in the absence of synaptic blockers. $^{*}p < 0.05$, $^{**}p < 0.01$, $^{***}p < 0.001$, $^{****}p < 0.0001$, n = 17 neurons for inhibitory only, 6 neurons for inhibitory followed by excitatory, and 12 neurons for excitatory only, two-way ANOVA followed by Bonferroni's comparisons test. C, 5-HT induced firing rate changes during the treatment and washout of 1 min in three different types of ZIR neurons in the absence of synaptic blockers. $^{*}p < 0.05$, $^{**}p < 0.01$, $^{***}p < 0.001$, $^{****}p < 0.0001$, n = 17 neurons for inhibitory only, 6 neurons for inhibitory followed by excitatory, and 12 neurons for excitatory only, two-way ANOVA followed by Bonferroni's comparisons test. D, 5-HT induced membrane potential changes during 5-HT treatment and washout of 1 min in three different types of ZIR neurons in the presence of synaptic blockers (AP5: 50 μM; CNQX: 10 μM; Bic: 30 μM). $^{*}p < 0.05$, $^{**}p < 0.01$, $^{****}p < 0.0001$, n = 10 neurons for inhibitory only, 3 neurons for inhibitory followed by excitatory, and 5 neurons for excitatory only, two-way ANOVA followed by Bonferroni's comparisons test. E, 5-HT induced firing rate changes during 5-HT treatment and washout of 1 min in three different types of ZIR neurons in the presence of synaptic blockers (AP5: 50 μM; CNQX: 10 μM; Bic: 30 μM). $^{*}p < 0.05$, $^{**}p < 0.01$, n = 10 neurons for inhibitory only, 3 neurons for inhibitory followed by excitatory, and 5 neurons for excitatory only, two-way ANOVA followed by Bonferroni's comparisons test. F, Percentages of ZIR neurons (n = 53) tested with inhibitory, inhibitory followed by excitatory, and excitatory effects by 5-HT application. G, A diagram showing that CTB-555 was injected into PVT to label presynaptic neurons in ZIR of GAD-GFP mice. H, A representative image shows CTB-positive fluorescence (purple) in the PVT targeted by stereotactic CTB injection. I, Retrogradely labelled CTB-positive neurons (I1) co-expressed with GAD-GFP (I2) in the ZIR with high colocalization (I3). J, Representative traces showing 5-HT (50 μM) inhibited one (above) but excited another (below) PVT-projecting CTB/GFP-positive ZIR neuron. K, Resting membrane potentials of PVT-projecting CTB/GFP-positive ZIR neurons before, during, and after 5-HT treatment. ns, no significance, $^{**}p < 0.01$, n = 14 neurons, RM one-way ANOVA followed by Bonferroni's multiple comparisons test. L, Separate data showing firing rates of PVT-projecting CTB/GFP-positive ZIR neurons with inhibitory only (n = 9 neurons) and delayed excitatory effects (n = 5 neurons) by 5-HT. ns, no significance, $^{*}p < 0.05$, $^{**}p < 0.01$, RM one-way ANOVA followed by Bonferroni's multiple comparisons test.

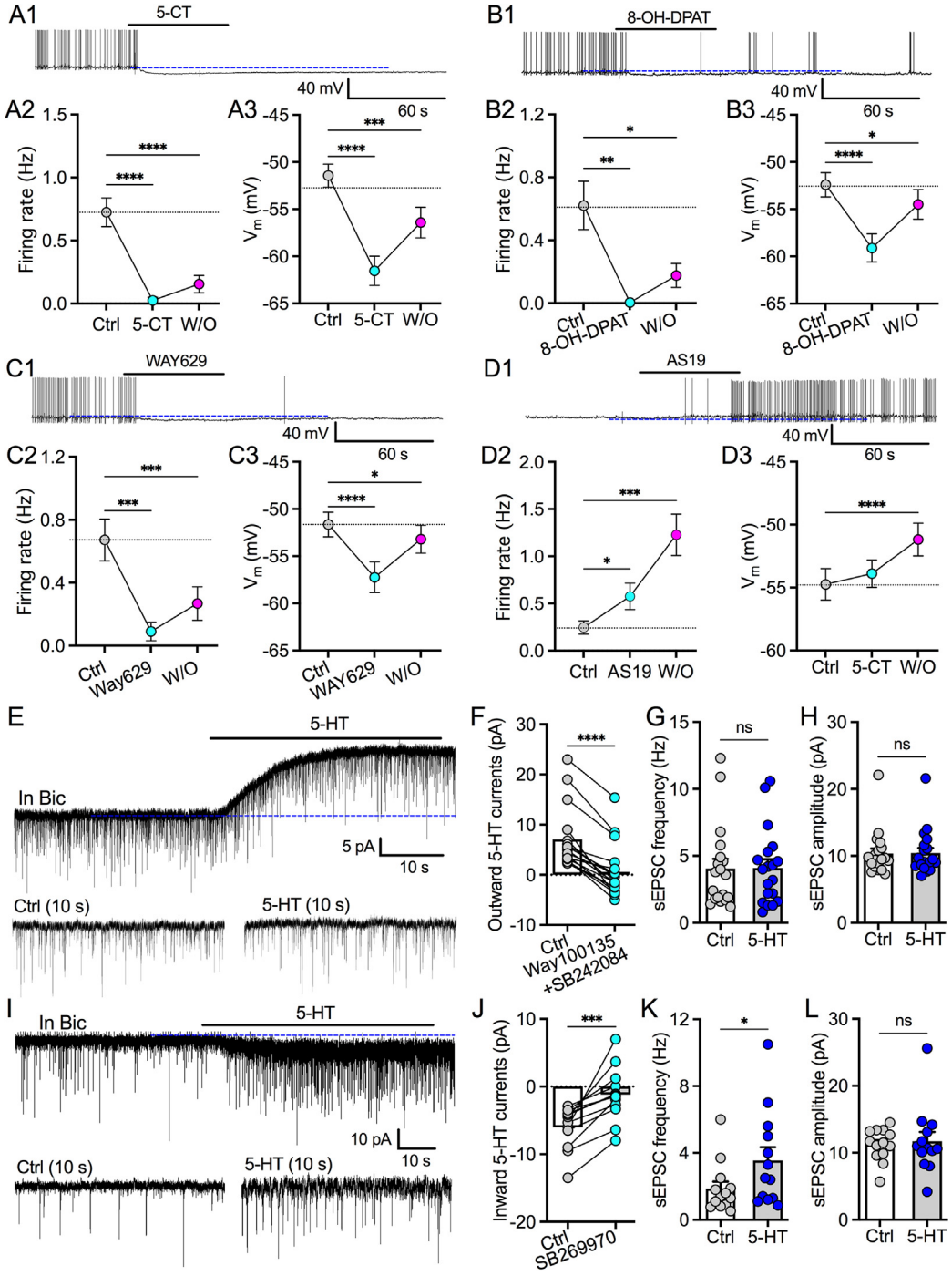

Figure 5: A combination of 5-HT receptor subtypes contributes to a bidirectional modulation of 5-HT on ZIR neurons. A1—A3, A representative trace (A1) and two symbol graphs show 5-CT (10 μM) decreased the firing rates (A2) and hyperpolarized the membrane potentials (A3) of ZIR neurons. ***$p < 0.001$, ****$p < 0.0001$, n = 23 neurons each group, RM one-way ANOVA. B1—B3, A representative trace (B1) and two symbol graphs show 8-OH-DPAT (10 μM) decreased the firing rates (B2) and hyperpolarized the membrane potentials (B3) of ZIR neurons. *$p < 0.05$, **$p < 0.01$, ****$p < 0.0001$, n = 18 neurons each group, RM one-way ANOVA. C1—C3, A representative trace (C1) and two symbol graphs show WAY-629 (10 μM) decreased the firing rates (C2) and hyperpolarized the membrane potentials (C3) of ZIR neurons. *$p < 0.05$, ***$p < 0.001$, ****$p < 0.0001$, n = 20 neurons each group, RM one-way ANOVA. D1-D3, A representative trace (D1) and two symbol graphs show AS19 (10 μM) increased the firing rates (D2) and depolorized the membrane potentials (D3) of ZIR neurons. *$p < 0.05$, ***$p < 0.001$, ****$p < 0.0001$, n = 21 neurons each group, RM one-way ANOVA. E, Representative traces indicate 5-HT evoked an outward current (top trace) without an effect on sEPSCs (bottom traces) in a ZIR neuron. F, A bar graph with data plots showing outward 5-HT currents were impaired by the application of Way100135 (10 μM) plus SB242084 (10 μM). ****$p < 0.0001$, n = 17 neurons each group, paired *t* test. G, 5-HT produced no effect on sEPSC frequency of 5-HT-inhibited ZIR neurons. ns, no significance, n = 19 neurons each group, paired *t* test. H, 5-HT had no effect on sEPSC amplitude of 5-HT-inhibited ZIR neurons in the presence of Bic (30 μM). ns, no significance, n = 19 neurons each group, paired *t* test. I, Representative traces show that 5-HT evoked an inward current (top trace) with increased sEPSC frequency (bottom traces) in a ZIR neuron. J, A bar graph with data plots showing inward 5-HT currents were reduced by the application of SB269970 (10 μM). ***$p < 0.001$, n = 12 neurons each group, paired *t* test. K, 5-HT increased sEPSC frequency of 5-HT-excited ZIR neurons in the presence of Bic (30 μM). *$p < 0.05$, n = 13 neurons each group, paired *t* test. L, 5-HT had no effect on sEPSC amplitude of 5-HT-excited ZIR neurons. ns, no significance, n = 13 neurons each group, paired *t* test.

HT, 5-CT produced long-lasting hyperpolarization to decrease firing rates of tested neurons (Figure 5A1—A3). These data suggest 5-CT may dominantly activate 5-HT1a or 5-HT2c to have inhibitory effect but not 5-HT7 for excitatory modulation. We then tested the effects of the selective 5-HT1a agonist 8-OH-DPAT and the selective 5-HT2c agonist WAY629 on the activity of ZIR neurons. Both 8-OH-DPAT (Figure 5B1—B3) and WAY629 (Figure 5C1—C3) inhibited the activity of ZIR neurons recorded. These data further support that both 5-HT1a and 5-HT2c contribute to 5-HT inhibition of ZIR neurons. In addition to 5-HT1a, 5-HT7 has been found in ZI [31]. Therefore, we also tested the effect of AS19, a selective 5-HT7 agonist, on the activity of ZIR neurons. We found AS19 depolarized ZIR neurons to produce a delayed and long-lasting excitatory effect (Figure 5D1—D3). Together, these data indicate a competitive effect of excitatory 5-HT7 and inhibitory 5-HT1a as well as 5-HT2c in ZIR neurons, supporting a receptor mechanism for a bidirectional 5-HT modulation.

Using voltage-clamp recording, we recorded both outward (Figure 5E) and inward (Figure 5I) currents evoked by 5-HT and tested the effect of selective 5-HT receptor antagonists. The outward currents were inhibited by the 5-HT1a antagonist WAY100635 together with the 5-HT2c antagonist SB242084 (Figure 5F). 5-HT had no effect on the frequency or the amplitude of spontaneous excitatory postsynaptic currents (sEPSCs) on ZIR neurons with outward 5-HT currents (Figure 5G,H). However, the inward 5-HT currents were abolished by SB269970, a selective 5-HT7 antagonist (Figure 5J). 5-HT also increased sEPSC frequency but not the amplitude on some ZIR neurons with inward 5-HT currents (Figure 5K and L). These data together further confirm that both 5-HT1a and 5-HT2c contribute to the inhibitory effect of 5-HT on ZIR neurons but 5-HT7 mediates the depolarization of 5-HT. In addition, 5-HT exerts the excitatory effect through both direct depolarization and an indirect mechanism to increase excitatory glutamate transmission onto ZIR neurons.

3.6. Acute fasting dynamically reduces 5-HT inhibition on ZIR GABA neurons

Previous studies have reported that fasting changed 5-HT turnover and decreased 5-HT2c expression in hypothalamus [27]. Here, we asked whether fasting over 24 h changes 5-HT modulation on ZIR GABA neurons. To examine the effect of 5-HT at various concentrations (0.5, 1, 5 and 50 μM), we recorded the activity of ZIR GAD-EGFP neurons in both regularly fed and 24-h fasted GAD-GFP mice (Figure 6A). Immunocytochemistry with GABA antibody confirmed that ZIR GAD67-GFP neurons expressed GABA (Figure 6B1—B3). 5-HT (50 μM) inhibited 53.1%, inhibited 25% with delayed excitation, and excited 21.9% of recorded ZIR GABA neurons from regularly fed mice (Figure 6C,E). In 24-h fasted mice, 5-HT (50 μM) inhibited only 22.6%, inhibited 35.5% with delayed excitation, and excited over 41.9% of ZIR GABA neurons recorded (Figure 6D,E). When all recorded neurons were included for statistical analysis, 5-HT (50 μM) produced strong hyperpolarization on ZIR GABA neurons in regularly fed mice but slight depolarization on neurons from 24-h fasted mice (Figure 6F). However, 5-HT (50 μM) had no effect on the mean firing rate of all recorded neurons from regularly fed mice but increased firing rate of neurons from 24-h fasted mice (Figure 6G). We also tested the effect of lower 5-HT doses and found 5-HT doses (0.5, 1 and 5 μM) all decreased firing rate of ZIR GABA neurons from regularly fed mice but produced no significant effect on neurons from fasted mice (Figure 6H,I). Together, these data indicate that low concentrations of 5-HT preferentially activate inhibitory 5-HT receptors to reduce the activity of ZIR GABA neurons in fed states, while increased 5-HT levels also induce an excitatory effect through activating excitatory 5-HT receptor subtypes. In the states of energy deficit following 24-h fasting, the inhibitory effect of 5-HT is downregulated that leads to an amplified increase in firing rate by higher 5-HT concentrations.

To examine whether the fasting-induced shift of 5-HT modulation on ZIR GABA neurons changes the regulation of raphe-ZIR 5-HT projections on food motivation in mice with energy deficit, we used PR trials to test the effect of photostimulation of raphe-ZIR 5-HT projections on operant behaviors for food reward in mice after 24 h fasting. We didn't detect an effect of photostimulation on active lever presses, breakpoints, or food reward retrieval (Figure 6J—L). These data together suggest activation of raphe-ZIR 5-HT projections has no conclusive effect on food motivation, which may be due to a complex and diverse effect of 5-HT modulation of ZIR neurons in different mice under fasted conditions.

3.7. Intermittent HFHS diet shifts the balance of 5-HT modulation from predominant inhibition to excitation

Our results above suggest that acute energy deficit shifts 5-HT effect on ZIR GABA neurons from inhibitory to excitatory. Here, we further tested whether intermittent HFHS diet, a model used to induce binge eating, changes 5-HT modulation on ZIR GABA neurons. Similarly, 5-HT (50 μM) produced bidirectional modulation with both inhibitory and excitatory effect on GABA neurons in both control and HFHS-diet mice (Figure 7A,B). When all neurons recorded were included for statistical analysis, 5-HT (50 μM) induced hyperpolarization to decrease firing rate of ZIR GABA neurons from mice with regular diet (Figure 7C,D) but evoked a small depolarization to excite neurons from mice with intermittent HFHS diet for 2—3 weeks (Figure 7C,E). We then separately analyzed the response of ZIR GABA neurons to 5-HT treatment. In control mice with regular chow, 5-HT (50 μM) inhibited 50.9% and excited 25.5% of ZIR GABA neurons recorded (Figure 7F—J). However, intermittent HFHS diet decreased the percentage of 5-HT-inhibited neurons to 31.5% but increased 5-HT-excited neurons to 44.8% (Figure 7F—J). These data thus indicate that intermittent HFHS diet shifts 5-HT effects from inhibition to excitation.

Similarly, we used PR trials to test the effect of raphe-ZIR 5-HT projection activation on motivation for food reward in mice treated with regular diet and intermittent HFHS food for 2—3 weeks. We found intermittent HFHS promoted reward earned during PR trials of 45 min (Figure 7M). Photostimulation of raphe-ZIR 5-HT projections significantly decreased active lever presses and reward consumption in control mice fed with regular diet but had little effect in mice with intermittent HFHS diet (Figure 7K—M). Together, these results suggest that intermittent HFHS diet downregulates 5-HT inhibition on ZIR GABA neurons and impairs the inhibitory regulation of raphe-ZIR 5-HT projections on food motivation.

3.8. Intermittent high-fat diet increases ZIR 5-HT7 expression

To further confirm 5-HT1a, 5-HT2c, and 5-HT7 expression in the ZIR, we used RNAscope in situ hybridization to detect mRNA levels of these receptor subtypes in regularly fed, 24-h fasted, and intermittent HFHS diet mice. We found high-level 5-HT1a and 5-HT2c mRNA expression in ZIR of mice without a significant difference among three group (Figure 8A1—B3, D1—E2, supplementary Figure 3). We also observed a low-level expression of 5-HT7 mRNA in ZIR and the density of the expression was increased by intermittent HFHS diet but not fasting (Figure 8C1—C6, F1—F2, supplementary Figure 3). These results thus suggest that increased 5-HT7 expression in ZIR may contribute to upregulated 5-HT excitation that contributes to less inhibitory control on feeding motivation and overeating of high-fat diet. In addition, we also

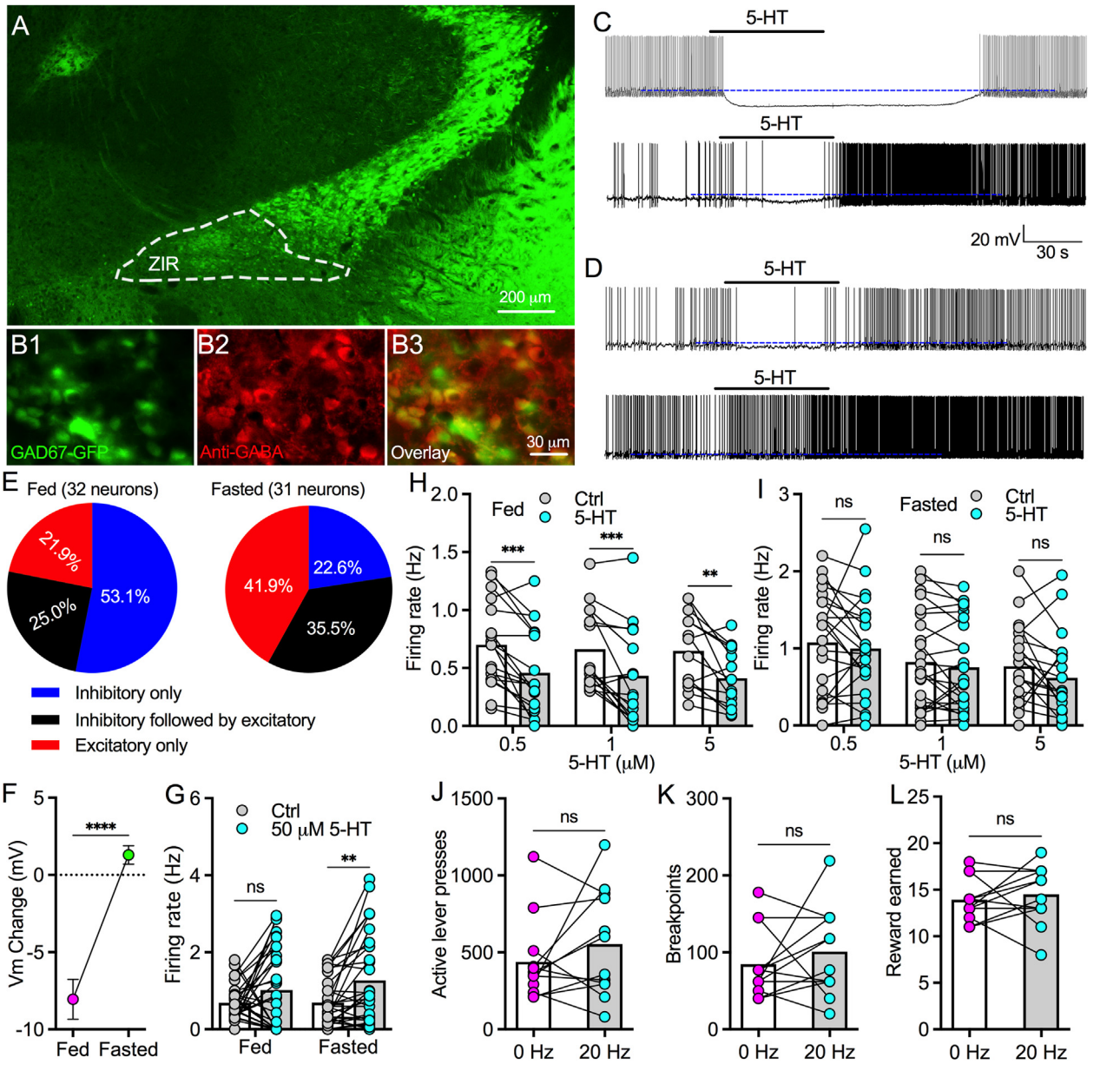

Figure 6: Fasting abolishes the inhibitory regulation of raphe-ZIR 5-HT signaling on ZIR GABA neurons and food motivation. A, Representative images showing ZIR GAD-GFP neurons from a GAD-GFP mouse used for recordings and testing 5-HT modulation on ZIR GABA neurons. B, Representative images shows GAD-GFP (*B1*), anti-GABA immunostaining (*B2*), and neurons co-expressed with both GFP and anti-GABA immunoreactivity (*B3*). C, Representative traces showing the effects of 5-HT (50 μM) on ZIR GAD-GFP neurons from slices of regularly fed mice. D, Representative traces showing the effects of 5-HT (50 μM) on ZIR GAD-GFP neurons from slices of 24-h fasted mice. E, Pie graphs showing percentages of recorded neurons that responded to 5-HT (50 μM) with inhibitory, inhibitory followed by excitatory, and excitatory effects in both regularly fed and 24-h fasted mice. F, 5-HT-induced changes of resting membrane potentials in neurons from both fed (n = 32 neurons) and fasted (n = 31 neurons) mice. $^{****}p < 0.0001$, paired t test. Unpaired t test. G, 5-HT (50 μM) had no effect statistically on firing rate of ZIR GABA neurons (n = 32) from regular fed mice but increased firing rate of neurons (n = 31) from 24-h fasted mice. The firing rate of 5-HT treatment was measured for a period of 2 min including 1-min application followed by 1-min washout. 5-HT effect: $F_{(1,61)} = 11.72$, $p = 0.0011$; fasting x 5-HT interaction: $F_{(1,61)} = 0.8424$, $p = 0.3623$; ns, no significance, $^{**}p < 0.01$, RM two-way ANOVA followed by Bonferroni's multiple comparisons test. H, 5-HT at 0.5 μM (n = 18 neurons), 1 μM (n = 17 neurons), and 5 μM (n = 14 neurons) decreased firing rate of ZIR GABA neurons from regular fed mice. The firing rate of 5-HT treatment was measured for a period of 2 min including 1-min application followed by 1-min washout. 5-HT effect: $F_{(1,46)} = 49.29$, $p < 0.0001$; dose x 5-HT interaction: $F_{(2,46)} = 0.0133$, $p = 0.9868$; $^{**}p < 0.01$, $^{***}p < 0.001$, RM two-way ANOVA followed by Bonferroni's multiple comparisons test. I, 5-HT at 0.5 μM (n = 23 neurons), 1 μM (n = 24 neurons), and 5 μM (n = 20 neurons) had no effect on firing rate of ZIR GABA neurons from 24-h fasted mice. 5-HT effect: $F_{(1,64)} = 3.70$, $p = 0.06$; dose x 5-HT interaction: $F_{(2,64)} = 0.2388$, $p = 0.7883$; ns, no significance, RM two-way ANOVA followed by Bonferroni's multiple comparisons test. The firing rate of 5-HT treatment was measured for a period of 2 min including 1-min application followed by 1-min washout. J, Bar graph with data plots showing active lever presses in 24-h fasted mice with and without photostimulation (20 Hz) of raphe-ZIR 5-HT projections. ns, no significance, n = 12 mice, paired *t* test. K, Breakpoints in 24-h fasted mice with and without photostimulation (20 Hz) of raphe-ZI 5-HT projections. ns, no significance, n = 12 mice, paired *t* test. L, Food reward earned by 24-h fasted mice with and without photostimulation (20 Hz) of raphe-ZI 5-HT projections. ns, no significance, n = 12 mice, paired *t* test.

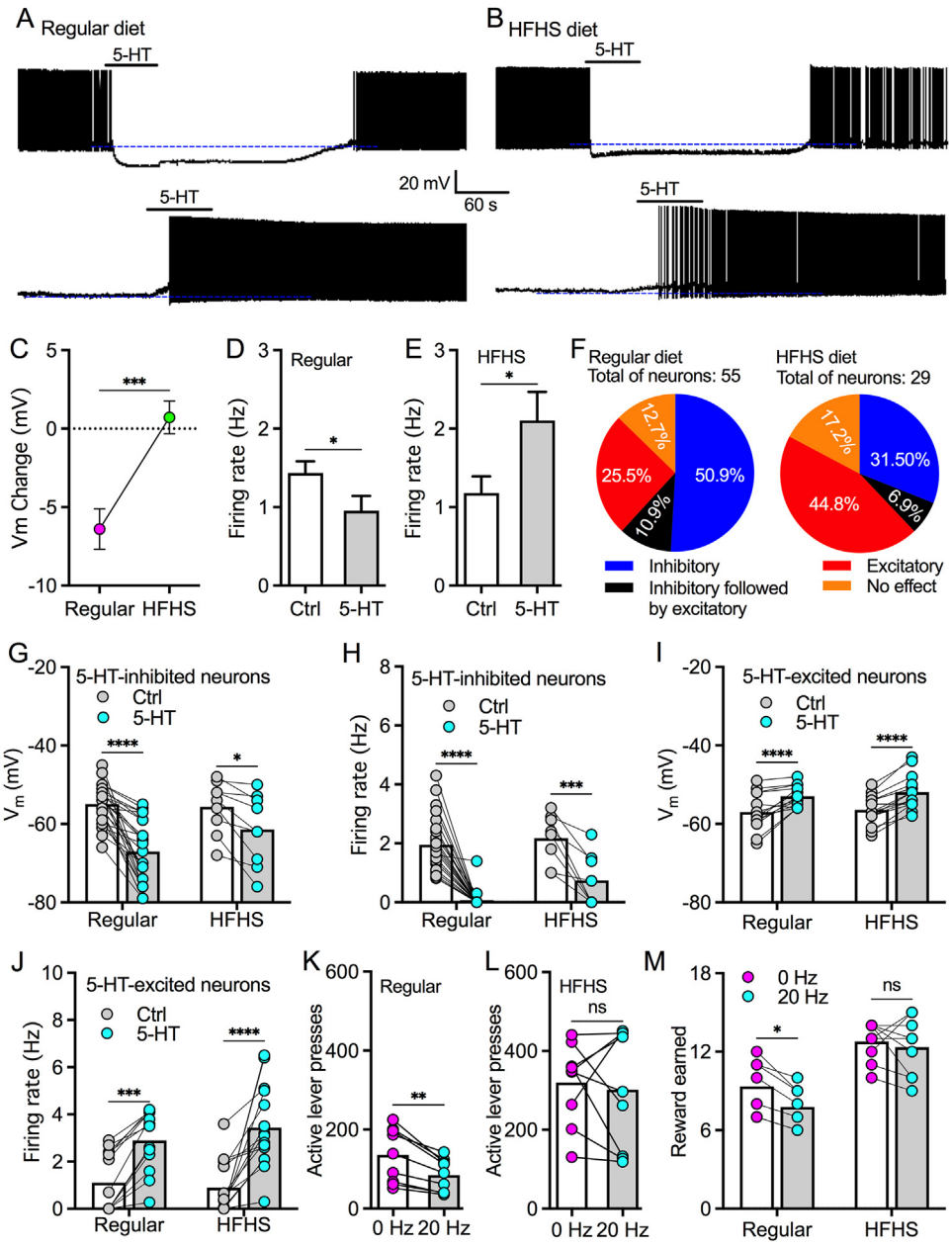

Figure 7: Intermittent HFHS diet attenuates the inhibitory regulation of raphe-ZIR 5-HT projections on food motivation. A, Representative traces show that 5-HT (50 μM) inhibited one ZIR GABA neuron but excited another ZIR GABA from a mouse treated with regular diet. B, Representative traces show that 5-HT (50 μM) inhibited one ZIR GABA neuron but excited another ZIR GABA from a mouse treated with intermittent HFHS diet. C, 5-HT-induced changes of resting membrane potentials in neurons from both regular (n = 55 neurons) and intermittent HFHS (n = 29 neurons) diets. $^{***}p < 0.001$, paired t test. Unpaired t test. D, A bar graph shows that 5-HT (50 μM) decreased firing rate of ZIR GABA neurons from mice with regular diet when all 55 neurons recorded were included for statistics. $^{*}p < 0.05$, paired t test. E, A bar graph shows that 5-HT (50 μM) increased firing rate of ZIR GABA neurons from mice with Intermittent HFHS diet when all 29 neurons recorded were included for statistics. $^{*}p < 0.05$, paired t test. F, Pie graphs showing percentages of recorded neurons that responded to 5-HT (50 μM) with inhibitory, inhibitory followed by excitatory, and excitatory effects in regular and HFHS-diet mice. G, 5-HT (50 μM) hyperpolarized majority of ZIR GABA neurons in mice with regular diet but a small percentage of ZIR GABA neurons from intermittent HFHS diet mice. 5-HT effect: $F_{(1,35)} = 41.38$, $p < 0.0001$; Diet x 5-HT interaction: $F_{(2,35)} = 5.24$, $p = 0.028$; $^{*}p < 0.05$, $^{****}p < 0.0001$, n = 28 neurons for mice with regular diet and 9 neurons for HFHS diet mice, RM two-way ANOVA. H, 5-HT (50 μM) decreased firing rate of the majority of ZIR GABA neurons in mice with regular diet and a small population of neurons from intermittent HFHS diet mice. 5-HT effect: $F_{(1,30)} = 68.27$, $p < 0.0001$; Diet x 5-HT interaction: $F_{(2,30)} = 1.25$, $p = 0.273$; $^{***}p < 0.001$, $^{****}p < 0.0001$, n = 24 neurons for mice with regular diet and 8 neurons for HFHS diet mice, RM two-way ANOVA. I, 5-HT (50 μM) depolarized a small population of ZIR GABA neurons from mice with regular diet but a majority of ZIR GABA neurons from intermittent HFHS diet mice. 5-HT effect: $F_{(1,27)} = 70.80$, $p < 0.0001$; Diet x 5-HT interaction: $F_{(2,27)} = 0.2153$, $p = 0.6463$; $^{****}p < 0.0001$, n = 14 neurons for mice with regular diet and 15 neurons for HFHS diet mice, RM two-way ANOVA. J, 5-HT (50 μM) increased firing rate of some ZIR GABA neurons from mice with regular diet but a large percentage of neurons from intermittent HFHS diet mice. 5-HT effect: $F_{(1,27)} = 58.40$, $p < 0.0001$; Diet x 5-HT interaction: $F_{(2,27)} = 1.821$, $p = 0.1884$; $^{***}p < 0.001$, $^{****}p < 0.0001$, n = 14 neurons for mice with regular diet and 15 neurons for HFHS diet mice, RM two-way ANOVA. K, Active lever presses by mice treated with regular chow during PR trials of 45 min $^{**}p < 0.01$, n = 9 mice, paired test. L, Active lever presses by mice treated with intermittent HFHS diet during PR trials of 45 min ns, no significance, n = 9 mice, paired test. M, HFHS pellet rewards earned by mice treated with regular chow and intermittent HFHS diet during PR trials of 45 min ns, no significance, $^{*}p < 0.05$, n = 9 mice each group, RM two-way ANOVA.

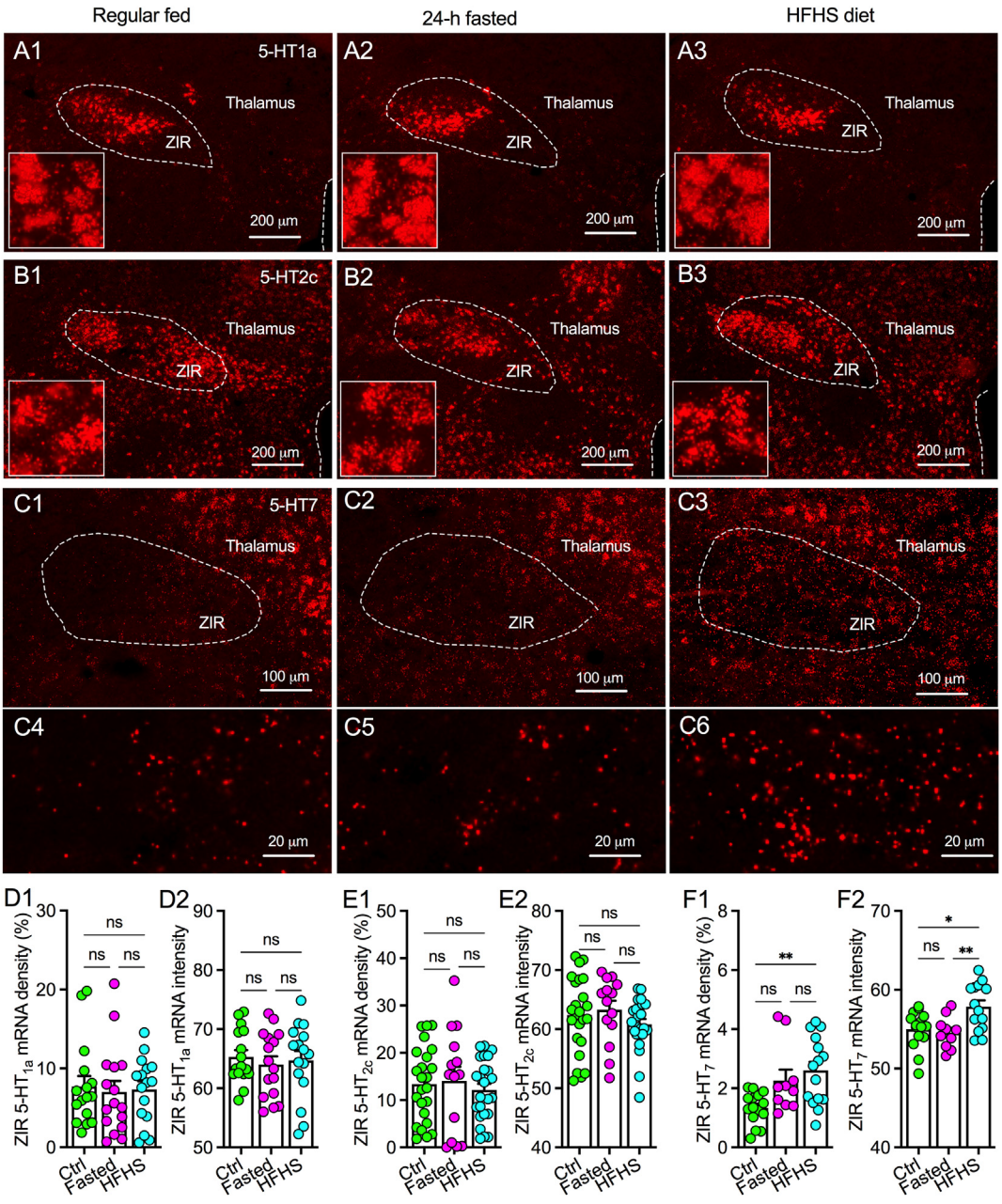

Figure 8: Patterns of 5-HT receptor subtype mRNA expression in ZIR of mice. A, Representative images showing 5-HT1a mRNA expression in the ZIR of mice with regular fed (*A1*), 24-h fasted (*A2*), and intermittent HFHS diet for 3 weeks (*A3*). Zoomed-in images were shown in the bottom left of each image. B, Representative images showing 5-HT2c mRNA expression in the ZIR of mice with regular fed (*B1*), 24-h fasted (*B2*), and intermittent HFHS diet for 3 weeks (*B3*). Zoomed-in images were shown in the bottom left of each image. C, Representative images showing 5-HT7 mRNA expression in the ZIR of mice with regular fed (*C1* and zoomed-in image *C4*), 24-h fasted (*C2* and zoomed-in image *C5*), and intermittent HFHS diet for 3 weeks (*C3* and zoomed-in image *C6*). D, Bar graphs with data plots showing both 5-HT1a density (*D1*) and intensity (*D2*) in ZIR of mice with regular fed (n = 16 ZIR areas from slices of 3 mice), 24-h fasted (n = 16 ZIR areas from slices of 3 mice, and intermittent HFHS diet for 3 weeks (n = 16 ZIR areas from slices of 3 mice). Treatment effect for mRNA density: $F_{(2,45)} = 0.076$, $p = 0.9267$. Treatment effect for mRNA intensity: $F_{(2,45)} = 0.218$, $p = 0.8052$, ns, no significance. E, Bar graphs with data plots showing both 5-HT2c density (*E1*) and intensity (*E2*) in ZIR of mice with regular fed (n = 24 ZIR areas from slices of 4 mice), 24-h fasted (n = 14 ZIR areas from slices of 3 mice, and intermittent HFHS diet for 3 weeks (n = 24 ZIR areas from slices of 4 mice). Treatment effect for mRNA density: $F_{(2,59)} = 0.274$, $p = 0.7610$. Treatment effect for mRNA intensity: $F_{(2,59)} = 0.990$, $p = 0.3773$, ns, no significance. F, Bar graphs with data plots showing both 5-HT7 density (*F1*) and intensity (*F2*) in ZIR of mice with regular fed (n = 15 ZIR areas from slices of 3 mice), 24-h fasted (n = 10 ZIR areas from slices of 2 mice, and intermittent HFHS diet for 3 weeks (n = 14 ZIR areas from slices of 3 mice). Treatment effect for mRNA density: $F_{(2,37)} = 6.807$, $p = 0.003$. Treatment effect for mRNA intensity: $F_{(2,37)} = 6.612$, $p = 0.004$, $^{*}p < 0.05$, $^{**}p < 0.01$, ns, no significance.

detected high-level of 5-HT7 and 5-HT2c but not 5-HT1a expression in the PVT (supplementary Figure 4), further supporting our previous finding about a dominant role of 5-HT7 in mediating 5-HT excitation of PVT neurons with slight inhibition mediated by 5-HT2c activation [30].

4. DISCUSSION

Here we report that raphe 5-HT neurons regulated feeding behavior through their projections to both ZI and PVT, the two regions connected

by inhibitory GABA neural circuits for the control of food intake [3]. Using retrograde AAV tracing, we found that 5-HT neurons in both DR and MnR nuclei projected to ZI and PVT. Interestingly, almost half of PVT-projecting raphe 5-HT neurons also collaterally innervated ZI. Although slice electrophysiological recordings showed a bidirectional modulation of 5-HT on ZIR GABA neurons, 5-HT concentrations lower than 50 μM and photostimulation of raphe-ZIR 5-HT projections predominantly inhibited ZIR neurons especially PVT-projecting ZIR GABA neurons in normal mice fed with regular diet. However, both 24-h fasting and intermittent HFHS diet shifted the bidirectional modulation of 5-HT on ZIR GABA neurons from a predominant inhibition to being excitation prone, which abolished the inhibitory effect of raphe-ZIR 5-HT signaling on feeding motivation.

The PVT was reported to regulate emotional expression and motivated behaviors including feeding by conveying neural signals from prefrontal cortex, ZI, and brain stem to limbic systems such as nucleus accumbens and amygdala [3,37,41–43]. Although PVT neurons are mainly glutamatergic, previous studies have revealed the diversity of PVT-based neural circuits in feeding control. Activation of PVT neurons produced either promoting or inhibitory effect on food motivation and consumption depending on PVT-originated circuitry connections [3,37,41,44,45]. In the present study, we found raphe 5-HT neurons send dense projections to PVT and activation of their axonal terminals excited PVT neurons to reduce food motivation and consumption. This is consistent with our latest report that the activity of raphe 5-HT neurons was inhibited by food deprivation [30]. Our previous study also revealed that 5-HT excited PVT neurons through activating 5-HT7 receptors and disinhibited these neurons by targeting 5-HT1a receptors in presynaptic GABAergic terminals [30]. Together, our findings support that both 5-HT1a and 5-HT7 receptors cooperatively work together to mediate feeding control by the raphe-PVT 5-HT signaling pathway.

The ZI is a critical brain area that sends GABA projections to inhibit PVT neurons for feeding control and acute activation of ZI-PVT GABA pathway evoked binge-like feeding behavior in seconds [3]. Despite an important role of ZI in the control of food intake, little is known about how ZI GABA neurons are innervated by other neural signals for feeding regulation. In the present study, we found raphe 5-HT neurons also innervate ZIR to modulate the activity of ZIR GABA neurons. Photostimulation of raphe-ZIR 5-HT projections predominantly inhibited ZIR neurons and reduced motivation for food reward. Previous studies have reported that DR 5-HT neurons project to both lateral geniculate body and superior colliculus with collateral axons for processing visual information [46]. The collateral 5-HT branching was also found to innervate both paraventricular nucleus of the hypothalamus (PVN) and lateral parabrachial nucleus (PBN) for autonomic control [47]. Using retrograde AAV for neural tracing, we found both DR and MnR 5-HT neurons sent projections to ZIR. On average, we labelled 47 neurons that projected to PVT but 287 neurons that projected to ZIR from five Sert-Cre mice. Despite a lower number of PVT-projecting 5-HT neurons were labelled which may be caused by low efficacy of either retrograde AAV or surgical targeting, half of these PVT-projecting neurons were found to send collateral axons to ZIR. Together, these findings suggest that a group of 5-HT neurons not only send projections to directly excite PVT neurons but also disinhibit PVT neurons through silencing presynaptic GABA neurons in the ZIR. The synchronous modulation of collateral 5-HT projections onto both presynaptic and postsynaptic neurons of ZI-PVT pathway is important for an efficient feeding control by a limited number of 5-HT neurons in the brain. Based on the property of the retrograde AAVs, they infect the axonal terminals of the injection sites and then are transported to the cell body for Cre-dependent expression of fluorescent proteins. However, the viruses are not able to differentiate the axons that terminate on PVT cell bodies or GABAergic terminals within PVT. Although half of PVT-projecting neurons were found to also send collateral axons to ZIR, it is not clear whether these collateral projections target PVT somas or GABAergic terminals from ZIR GABA neurons.

5-HT receptor signaling in multiple brain areas was reported to regulate food intake. Both 5-HT1b in agouti-related peptide (AgPR) neurons and 5-HT2c in proopiomelanocortin (POMC) neurons of the arcuate nucleus (ARC) contribute to 5-HT inhibition of homeostatic feeding [13,48,49]. In addition to ARC, both VTA and nucleus of the solitary tract (NTS) also express 5-HT2c receptors to mediate the inhibitory regulation of 5-HT on food intake [20,50,51]. Although activation of 5-HT2c in brain areas above tend to reduce food intake, it also promotes feeding when PVN 5-HT2c receptors are activated by 5-HT signaling [21]. These findings thus suggest a complex role of 5-HT neural projections in the regulation of food intake. Together with our previous report, activation of raphe-PVT 5-HT signaling inhibited food motivation through acting on both 5-HT1a and 5-HT7 receptors in the PVT. However, in the ZI, 5-HT exerted a bidirectional modulation on ZI GABA neurons though it predominantly inhibited these neurons in well fed conditions. The present findings indicate that 5-HT inhibited ZIR GABA neurons by activating both 5-HT1a and 5-HT2c receptors but excited them through the action on 5-HT7 subtypes. 5-HT2c was traditionally considered as an excitatory receptor but it was recently reported to also mediate an inhibitory effect of 5-HT on PVN neurons [21]. Consistent with this report, 5-HT2c participated in the inhibitory effect of 5-HT on ZIR GABA neurons. Together with our previous findings about 5-HT modulation on PVT neurons [30], the present study indicates that 5-HT1a is expressed not only in the soma but also the PVT terminals of ZI GABA neurons to disinhibit PVT neurons for feeding inhibition when collateral 5-HT projections are activated. However, activation of ZI 5-HT7 receptors may antagonize the excitatory effect of PVT 5-HT7 signaling on PVT neurons for feeding control. Thus, our findings further confirm the complexity and diversity of 5-HT receptor subtypes in the regulation of food intake.

Changes in central 5-HT modulation are considered to be involved in the development of obesity and reduced postprandial 5-HT signaling results in insufficient inhibition of additional food intake. Previous studies were predominantly focused on presynaptic mechanism related to changes in 5-HT release and reuptake induced by fasting and high-fat diet. In humans, high-fat diet decreases 5-HT transporter (SERT) binding in the hypothalamus and 24-h fasting increases hypothalamic SERT availability in lean brains [52,53]. In rodents, high-fat diet also decreased 5-HT levels in the hypothalamus [54]. The fasting-induced increase in hypothalamic SERT availability in the lean healthy subjects likely reflects increased SERT affinity induced by decreased synaptic 5-HT levels [55,56], contributing to a promoting effect in food seeking and consumption [57]. However, fasting-induced increase in SERT binding was absent in men with obesity [52], suggesting a blunted 5-HT signaling in the development of obesity. Our previous study has reported that intermittent HFHS diet impaired both 5-HT inhibition of ZIR-PVT GABA transmission and 5-HT activation of PVT neurons [30]. These findings thus suggest that HFHS-diet-induced downregulation in 5-HT inhibition of ZIR-PVT GABA transmission leads to a disinhibition of PVT neurons for diet-induced overeating. In the present study, we found both 5-HT treatment and photostimulation of raphe-ZIR 5-HT terminals modulated the activity of ZIR neurons. Although 5-HT exerted a bidirectional modulation with both inhibitory and excitatory effects on ZIR GABA neurons in mice well fed with regular food, it predominantly inhibited ZIR GABA neurons especially

PVT-projecting ZIR GABA neurons. However, in 24-h fasted mice and mice with intermittent HFHS diet, more ZIR GABA neurons were excited by 5-HT that led to a slightly excitatory effect on a general population of ZIR GABA neurons. These findings together indicate that postsynaptic 5-HT modulation of ZIR GABA neurons was changed by both fasting and intermittent HFHS diet, which shifted the balance of 5-HT modulation from predominant inhibition to less inhibition or even slight excitation. Based on the promoting effect on food intake mediated by activation of ZIR GABA neurons and their projections to PVT, fasting-induced decrease in 5-HT inhibition of these neurons contributes to an increased activation of ZIR-PVT GABA transmission that promotes feeding motivation in the condition of energy deficit. However, HFHS-diet-induced downregulation of 5-HT signaling in ZIR GABA neurons leads to an overactivation of ZIR-PVT pathway that develops diet-induced overeating and obesity. These possibilities were supported by our results that optogenetic activation of raphe-ZIR 5-HT projections had little effect on food motivation in both 24-h fasted mice and mice with intermittent HFHS diet for 2—3 weeks. Together with our previous report about HFHS-diet-induced downregulation in 5-HT inhibition of ZIR-PVT GABA release, the present study further confirms that dynamic 5-HT signaling tunes ZIR-PVT GABA transmission for both controlling daily food intake and causing diet-induced overeating.

Our RNAscope assay confirmed that ZIR expressed high levels of both 5-HT1a and 5-HT2c mRNA as well as low level of 5-HT7 mRNA. These data are consistent with our electrophysiological data about a predominant inhibitory effect of 5-HT on the activity of ZIR neurons through activation of both 5-HT1a and 5-HT2c receptors. Especially, 5-HT1a mRNA were selectively expressed in lateral ZIR, the major origin of PVT-projecting GABA neurons for feeding control [3]. Furthermore, we found intermittent HFHS diet but not 24-h fasting increased the density and intensity of 5-HT7 mRNA expression in ZIR. However, we didn't observe any effect on 5-HT1a and 5-HT2c mRNA expression by fasting and intermittent HFHS diet. These findings thus suggested that increased 5-HT7 receptor levels may contribute to an increased 5-HT excitation of ZIR GABA neurons for less inhibition on food motivation. However, the exact mechanism for decreased 5-HT inhibition on these neurons remains unclear. Both endocytosis and intracellular trafficking were found to regulate the level of functional 5-HT1a receptors in the neuronal membrane [58—61]. Previous studies have also reported that both stress and alcohol exposure change the expression and the membrane localization of postsynaptic 5-HT receptors through the regulation in trafficking and internalization [62—67]. Whether fasting and HFHS diet regulate the process for 5-HT receptor trafficking and internalization for changing postsynaptic 5-HT modulation should be studied in future studies.

As discussed above, photostimulation of ZIR 5-HT axons had little effect on feeding in mice after 24 h fasting. However, despite a fasting-induced reduction in 5-HT inhibition of ZIR-PVT GABA transmission, photostimulation of PVT 5-HT projections still depressed feeding motivation in fasted mice. These findings thus suggest that 5-HT axons not only target presynaptic ZIR GABA terminals in PVT but also directly innervate PVT neurons, which is also supported by our electrophysiological data with photostimulation of PVT 5-HT terminals. Although 5-HT-induced disinhibition by targeting ZIR GABA terminals is reduced by fasting, photostimulation of PVT 5-HT projections can still depress feeding behavior by releasing 5-HT to directly excite PVT neurons. Therefore, these results further confirm that raphe-PVT 5-HT projections regulate feeding behavior through both direct excitation of PVT neurons and indirect disinhibition that targeting ZIR-PVT GABA terminals.

In conclusion, our results show that raphe 5-HT neurons send projections to both ZIR and PVT for the regulation of food intake. A dynamic modulation of 5-HT signaling on PVT-projecting ZIR GABA neurons reveals that transient reduction in ZIR 5-HT inhibition authorizes daily food intake but sustained change of ZIR 5-HT signaling leads to overeating induced by HFHS diet. In addition, half of PVT-projecting 5-HT neurons also send collateral axons to ZIR, suggesting PVT 5-HT projections regulate feeding behavior not only through a direct excitation of PVT neurons but also by targeting ZIR-PVT GABAergic terminals for an indirect disinhibition.

FUNDING

This work was supported by the NIH grant R01 DK131441 and Florida State University Startup to X.Z.

AUTHOR CONTRIBUTIONS

X.Z. conceived the project and designed the experiments. Q.Y., J.N., and X.Z. performed the experiments and analyzed the data. X.Z wrote the paper and all authors approved the final version of the manuscript.

DATA AVAILABILITY

Data will be made available on request.

ACKNOWLEDGMENTS

We appreciate Drs. Linda Rinaman and Huiyuan Zheng, as well as Natalia Valderrama for the technical assistance in RNAscope in situ hybridization. We thank Harley Beach for her discussion and critical reading of the manuscript.

CONFLICT OF INTEREST

The authors declare no competing interests.

APPENDIX A. SUPPLEMENTARY DATA

Supplementary data to this article can be found online at https://doi.org/10.1016/j.molmet.2022.101634.

REFERENCES

[1] Ogasawara, T., Sogukpinar, F., Zhang, K., Feng, Y.Y., Pai, J., Jezzini, A., et al., 2022. A primate temporal cortex-zona incerta pathway for novelty seeking. Nat Neurosci 25:50—60.

[2] Ahmadlou, M., Houba, J.H.W., van Vierbergen, J.F.M., Giannouli, M., Gimenez, G.A., van Weeghel, C., et al., 2021. A cell type-specific cortico-subcortical brain circuit for investigatory and novelty-seeking behavior. Science 372.

[3] Zhang, X., van den Pol, A.N., 2017. Rapid binge-like eating and body weight gain driven by zona incerta GABA neuron activation. Science 356:853—859.

[4] Zhao, Z.D., Chen, Z., Xiang, X., Hu, M., Xie, H., Jia, X., et al., 2019. Zona incerta GABAergic neurons integrate prey-related sensory signals and induce an appetitive drive to promote hunting. Nat Neurosci 22:921—932.

[5] Liu, K., Kim, J., Kim, D.W., Zhang, Y.S., Bao, H., Denaxa, M., et al., 2017. Lhx6-positive GABA-releasing neurons of the zona incerta promote sleep. Nature 548:582—587.

[6] Venkataraman, A., Brody, N., Reddi, P., Guo, J., Gordon Rainnie, D., Dias, B.G., 2019. Modulation of fear generalization by the zona incerta. Proc Natl Acad Sci U S A 116:9072—9077.

[7] Li, Z., Rizzi, G., Tan, K.R., 2021. Zona incerta subpopulations differentially encode and modulate anxiety. Sci Adv 7:eabf6709.

[8] Shang, C., Liu, A., Li, D., Xie, Z., Chen, Z., Huang, M., et al., 2019. A subcortical excitatory circuit for sensory-triggered predatory hunting in mice. Nat Neurosci 22:909–920.
[9] Zahodne, L.B., Susatia, F., Bowers, D., Ong, T.L., Jacobson, C.E.t., Okun, M.S., et al., 2011. Binge eating in Parkinson's disease: prevalence, correlates and the contribution of deep brain stimulation. J Neuropsychiatry Clin Neurosci 23: 56–62.
[10] Amami, P., Dekker, I., Piacentini, S., Ferre, F., Romito, L.M., Franzini, A., et al., 2015. Impulse control behaviours in patients with Parkinson's disease after subthalamic deep brain stimulation: de novo cases and 3-year follow-up. J Neurol Neurosurg Psychiatry 86:562–564.
[11] Novakova, L., Haluzik, M., Jech, R., Urgosik, D., Ruzicka, F., Ruzicka, E., 2011. Hormonal regulators of food intake and weight gain in Parkinson's disease after subthalamic nucleus stimulation. Neuroendocrinol Lett 32:437–441.
[12] Lechin, F., van der Dijs, B., Hernandez-Adrian, G., 2006. Dorsal raphe vs. median raphe serotonergic antagonism. Anatomical, physiological, behavioral, neuroendocrinological, neuropharmacological and clinical evidences: relevance for neuropharmacological therapy. Prog Neuro-Psychopharmacol Biol Psychiatry 30:565–585.
[13] He, Y., Cai, X., Liu, H., Conde, K.M., Xu, P., Li, Y., et al., 2021. 5-HT recruits distinct neurocircuits to inhibit hunger-driven and non-hunger-driven feeding. Mol Psychiatr 26:7211–7224.
[14] Zhang, H., Li, K., Chen, H.S., Gao, S.Q., Xia, Z.X., Zhang, J.T., et al., 2018. Dorsal raphe projection inhibits the excitatory inputs on lateral habenula and alleviates depressive behaviors in rats. Brain Struct Funct 223:2243–2258.
[15] Paquelet, G.E., Carrion, K., Lacefield, C.O., Zhou, P., Hen, R., Miller, B.R., 2022. Single-cell activity and network properties of dorsal raphe nucleus serotonin neurons during emotionally salient behaviors. Neuron.
[16] Courtiol, E., Menezes, E.C., Teixeira, C.M., 2021. Serotonergic regulation of the dopaminergic system: implications for reward-related functions. Neurosci Biobehav Rev 128:282–293.
[17] Miyazaki, K., Miyazaki, K.W., Sivori, G., Yamanaka, A., Tanaka, K.F., Doya, K., 2020. Serotonergic projections to the orbitofrontal and medial prefrontal cortices differentially modulate waiting for future rewards. Sci Adv 6.
[18] Abela, A.R., Browne, C.J., Sargin, D., Prevot, T.D., Ji, X.D., Li, Z., et al., 2020. Median raphe serotonin neurons promote anxiety-like behavior via inputs to the dorsal hippocampus. Neuropharmacology 168:107985.
[19] Xu, Y., Jones, J.E., Kohno, D., Williams, K.W., Lee, C.E., Choi, M.J., et al., 2008. 5-HT2CRs expressed by pro-opiomelanocortin neurons regulate energy homeostasis. Neuron 60:582–589.
[20] Xu, P., He, Y., Cao, X., Valencia-Torres, L., Yan, X., Saito, K., et al., 2017. Activation of serotonin 2C receptors in dopamine neurons inhibits binge-like eating in mice. Biol Psychiatr 81:737–747.
[21] Yoo, E.S., Li, L., Jia, L., Lord, C.C., Lee, C.E., Birnbaum, S.G., et al., 2021. Galphai/o-coupled Htr2c in the paraventricular nucleus of the hypothalamus antagonizes the anorectic effect of serotonin agents. Cell Rep 37:109997.
[22] Belmer, A., Patkar, O.L., Pitman, K.M., Bartlett, S.E., 2016. Serotonergic neuroplasticity in alcohol addiction. Brain Plast 1:177–206.
[23] Bailer, U.F., Frank, G.K., Henry, S.E., Price, J.C., Meltzer, C.C., Weissfeld, L., et al., 2005. Altered brain serotonin 5-HT1A receptor binding after recovery from anorexia nervosa measured by positron emission tomography and [carbonyl11C]WAY-100635. Arch Gen Psychiatr 62:1032–1041.
[24] Bailer, U.F., Bloss, C.S., Frank, G.K., Price, J.C., Meltzer, C.C., Mathis, C.A., et al., 2011. 5-HT(1)A receptor binding is increased after recovery from bulimia nervosa compared to control women and is associated with behavioral inhibition in both groups. Int J Eat Disord 44:477–487.
[25] Kaye, W.H., Frank, G.K., Bailer, U.F., Henry, S.E., Meltzer, C.C., Price, J.C., et al., 2005. Serotonin alterations in anorexia and bulimia nervosa: new insights from imaging studies. Physiol Behav 85:73–81.
[26] Bailer, U.F., Frank, G.K., Henry, S.E., Price, J.C., Meltzer, C.C., Mathis, C.A., et al., 2007. Exaggerated 5-HT1A but normal 5-HT2A receptor activity in individuals ill with anorexia nervosa. Biol Psychiatr 61:1090–1099.
[27] Wang, H., Huang, Z., Huang, L., Niu, S., Rao, X., Xu, J., et al., 2012. Hypothalamic Ahi1 mediates feeding behavior through interaction with 5-HT2C receptor. J Biol Chem 287:2237–2246.
[28] Nonogaki, K., Nozue, K., Oka, Y., 2006. Hyperphagia alters expression of hypothalamic 5-HT2C and 5-HT1B receptor genes and plasma des-acyl ghrelin levels in Ay mice. Endocrinology 147:5893–5900.
[29] Gur, E., Newman, M.E., Avraham, Y., Dremencov, E., Berry, E.M., 2003. The differential effects of food restriction on 5-HT1A and 5-HT1B receptor mediated control of serotonergic transmission in the hippocampus and hypothalamus of rats. Nutr Neurosci 6:169–175.
[30] Ye, Q., Zhang, X., 2021. Serotonin activates paraventricular thalamic neurons through direct depolarization and indirect disinhibition from zona incerta. J Physiol 599:4883–4900.
[31] Siddiqui, A., Abu-Amara, M., Aldairy, C., Hagan, J.J., Wilson, C., 2004. 5-HT7 receptor subtype as a mediator of the serotonergic regulation of luteinizing hormone release in the zona incerta. Eur J Pharmacol 491:77–84.
[32] Goel, N., Innala, L., Viau, V., 2014. Sex differences in serotonin (5-HT) 1A receptor regulation of HPA axis and dorsal raphe responses to acute restraint. Psychoneuroendocrinology 40:232–241.
[33] Siddiqui, A., Kotecha, K., Salicioni, A.M., Kalia, V., Murray, J.F., Wilson, C.A., 2000. Serotonin inhibits luteinizing hormone release via 5-HT1A receptors in the zona incerta of ovariectomised, anaesthetised rats primed with steroids. Neuroendocrinology 72:272–283.
[34] Zhuang, X., Masson, J., Gingrich, J.A., Rayport, S., Hen, R., 2005. Targeted gene expression in dopamine and serotonin neurons of the mouse brain. J Neurosci Methods 143:27–32.
[35] Vong, L., Ye, C., Yang, Z., Choi, B., Chua Jr., S., Lowell, B.B., 2011. Leptin action on GABAergic neurons prevents obesity and reduces inhibitory tone to POMC neurons. Neuron 71:142–154.
[36] Tamamaki, N., Yanagawa, Y., Tomioka, R., Miyazaki, J., Obata, K., Kaneko, T., 2003. Green fluorescent protein expression and colocalization with calretinin, parvalbumin, and somatostatin in the GAD67-GFP knock-in mouse. J Comp Neurol 467:60–79.
[37] Barrett, L.R., Nunez, J., Zhang, X., 2021. Oxytocin activation of paraventricular thalamic neurons promotes feeding motivation to attenuate stress-induced hypophagia. Neuropsychopharmacology 46:1045–1056.
[38] Zheng, H., Reiner, D.J., Hayes, M.R., Rinaman, L., 2019. Chronic suppression of glucagon-like peptide-1 receptor (GLP1R) mRNA translation in the rat bed nucleus of the stria terminalis reduces anxiety-like behavior and stress-induced hypophagia, but prolongs stress-induced elevation of plasma corticosterone. J Neurosci 39:2649–2663.
[39] Schindelin, J., Arganda-Carreras, I., Frise, E., Kaynig, V., Longair, M., Pietzsch, T., et al., 2012. Fiji: an open-source platform for biological-image analysis. Nat Methods 9:676–682.
[40] Yang, T., Poenisch, M., Khanal, R., Hu, Q., Dai, Z., Li, R., et al., 2021. Therapeutic HNF4A mRNA attenuates liver fibrosis in a preclinical model. J Hepatol 75:1420–1433.
[41] Ye, Q., Nunez, J., Zhang, X., 2022. Oxytocin receptor-expressing neurons in the paraventricular thalamus regulate feeding motivation through excitatory projections to the nucleus accumbens core. J Neurosci 42:3949–3964.
[42] Hsu, D.T., Kirouac, G.J., Zubieta, J.K., Bhatnagar, S., 2014. Contributions of the paraventricular thalamic nucleus in the regulation of stress, motivation, and mood. Front Behav Neurosci 8:73.
[43] Christoffel, D.J., Walsh, J.J., Heifets, B.D., Hoerbelt, P., Neuner, S., Sun, G., et al., 2021. Input-specific modulation of murine nucleus accumbens differentially regulates hedonic feeding. Nat Commun 12:2135.

[44] Labouebe, G., Boutrel, B., Tarussio, D., Thorens, B., 2016. Glucose-responsive neurons of the paraventricular thalamus control sucrose-seeking behavior. Nat Neurosci 19:999—1002.

[45] Zhang, J., Chen, D., Sweeney, P., Yang, Y., 2020. An excitatory ventromedial hypothalamus to paraventricular thalamus circuit that suppresses food intake. Nat Commun 11:6326.

[46] Villar, M.J., Vitale, M.L., Hokfelt, T., Verhofstad, A.A., 1988. Dorsal raphe serotoninergic branching neurons projecting both to the lateral geniculate body and superior colliculus: a combined retrograde tracing-immunohistochemical study in the rat. J Comp Neurol 277:126—140.

[47] Petrov, T., Krukoff, T.L., Jhamandas, J.H., 1992. The hypothalamic paraventricular and lateral parabrachial nuclei receive collaterals from raphe nucleus neurons: a combined double retrograde and immunocytochemical study. J Comp Neurol 318:18—26.

[48] Heisler, L.K., Jobst, E.E., Sutton, G.M., Zhou, L., Borok, E., Thornton-Jones, Z., et al., 2006. Serotonin reciprocally regulates melanocortin neurons to modulate food intake. Neuron 51:239—249.

[49] Sohn, J.W., Xu, Y., Jones, J.E., Wickman, K., Williams, K.W., Elmquist, J.K., 2011. Serotonin 2C receptor activates a distinct population of arcuate pro-opiomelanocortin neurons via TRPC channels. Neuron 71:488—497.

[50] D'Agostino, G., Lyons, D., Cristiano, C., Lettieri, M., Olarte-Sanchez, C., Burke, L.K., et al., 2018. Nucleus of the solitary tract serotonin 5-HT2C receptors modulate food intake. Cell Metabol 28:619—630 e615.

[51] Valencia-Torres, L., Olarte-Sanchez, C.M., Lyons, D.J., Georgescu, T., Greenwald-Yarnell, M., Myers Jr., M.G., et al., 2017. Activation of ventral tegmental area 5-HT2C receptors reduces incentive motivation. Neuropsychopharmacology 42:1511—1521.

[52] van Galen, K.A., Booij, J., Schrantee, A., Adriaanse, S.M., Unmehopa, U.A., Fliers, E., et al., 2021. The response to prolonged fasting in hypothalamic serotonin transporter availability is blunted in obesity. Metabolism 123:154839.

[53] Koopman, K.E., Booij, J., Fliers, E., Serlie, M.J., la Fleur, S.E., 2013. Diet-induced changes in the Lean Brain: hypercaloric high-fat-high-sugar snacking decreases serotonin transporters in the human hypothalamic region. Mol Metabol 2:417—422.

[54] Haleem, D.J., Mahmood, K., 2021. Brain serotonin in high-fat diet-induced weight gain, anxiety and spatial memory in rats. Nutr Neurosci 24:226—235.

[55] Innis, R.B., Cunningham, V.J., Delforge, J., Fujita, M., Gjedde, A., Gunn, R.N., et al., 2007. Consensus nomenclature for in vivo imaging of reversibly binding radioligands. J Cerebr Blood Flow Metabol 27:1533—1539.

[56] Grouleff, J., Ladefoged, L.K., Koldso, H., Schiott, B., 2015. Monoamine transporters: insights from molecular dynamics simulations. Front Pharmacol 6:235.

[57] Lam, D.D., Garfield, A.S., Marston, O.J., Shaw, J., Heisler, L.K., 2010. Brain serotonin system in the coordination of food intake and body weight. Pharmacol Biochem Behav 97:84—91.

[58] Kumar, G.A., Sarkar, P., Jafurulla, M., Singh, S.P., Srinivas, G., Pande, G., et al., 2019. Exploring endocytosis and intracellular trafficking of the human Serotonin1A receptor. Biochemistry 58:2628—2641.

[59] Riad, M., Watkins, K.C., Doucet, E., Hamon, M., Descarries, L., 2001. Agonist-induced internalization of serotonin-1a receptors in the dorsal raphe nucleus (autoreceptors) but not hippocampus (heteroreceptors). J Neurosci 21:8378—8386.

[60] Zimmer, L., Riad, M., Rbah, L., Belkacem-Kahlouli, A., Le Bars, D., Renaud, B., et al., 2004. Toward brain imaging of serotonin 5-HT1A autoreceptor internalization. Neuroimage 22:1421—1426.

[61] Bouaziz, E., Emerit, M.B., Vodjdani, G., Gautheron, V., Hamon, M., Darmon, M., et al., 2014. Neuronal phenotype dependency of agonist-induced internalization of the 5-HT(1A) serotonin receptor. J Neurosci 34:282—294.

[62] Ferguson, S.M., Sandygren, N.A., Neumaier, J.F., 2009. Pairing mild stress with increased serotonin-1B receptor expression in the nucleus accumbens increases susceptibility to amphetamine. Eur J Neurosci 30:1576—1584.

[63] Darmon, M., Al Awabdh, S., Emerit, M.B., Masson, J., 2015. Insights into serotonin receptor trafficking: cell membrane targeting and internalization. Prog Mol Biol Transl Sci 132:97—126.

[64] Wang, S., Liu, H., Roberts, J.B., Wiley, A.P., Marayati, B.F., Adams, K.L., et al., 2022. Prolonged ethanol exposure modulates constitutive internalization and recycling of 5-HT1A receptors. J Neurochem 160:469—481.

[65] Luessen, D.J., Sun, H., McGinnis, M.M., Hagstrom, M., Marrs, G., McCool, B.A., et al., 2019. Acute ethanol exposure reduces serotonin receptor 1A internalization by increasing ubiquitination and degradation of beta-arrestin2. J Biol Chem 294:14068—14080.

[66] Burnett, E.J., Grant, K.A., Davenport, A.T., Hemby, S.E., Friedman, D.P., 2014. The effects of chronic ethanol self-administration on hippocampal 5-HT1A receptors in monkeys. Drug Alcohol Depend 136:135—142.

[67] Al Awabdh, S., Miserey-Lenkei, S., Bouceba, T., Masson, J., Kano, F., Marinach-Patrice, C., et al., 2012. A new vesicular scaffolding complex mediates the G-protein-coupled 5-HT1A receptor targeting to neuronal dendrites. J Neurosci 32:14227—14241.

